European Journal of Taxonomy 1001: 1–51
https://doi.org/10.5852/ejt.2025.1001.2951

ISSN 2118-9773
www.europeanjournaloftaxonomy.eu
2025 · Jaume-Schinkel S. *et al.*

Monograph

urn:lsid:zoobank.org:pub:1726F665-E94D-45CD-83DC-3102CE2C1C50

Revision of the genus *Bryopharsos* Quate, 1996 (Diptera: Psychodidae) with the description of nine new species

Santiago JAUME-SCHINKEL [1,*], Isabel C. KILIAN [2], Alex PAZMIÑO-PALOMINO [3] & Ximo MENGUAL [4]

[1,2,4] Museum Koenig, Leibniz-Institut zur Analyse des Biodiversitätswandels, Adenauerallee 127, D-53113 Bonn, Germany.
[2] Department of Agroecology and Organic Farming, Institute of Crop Science and Resource Conservation, Faculty of Agriculture, University of Bonn, Auf dem Hügel 6, D-53121 Bonn, Germany.
[1,3,4] Instituto Nacional de Biodiversidad, División de Entomología. Rumipamba N341 y Av. Los Shyris, 170506 Quito, Ecuador.
[3] Museo de Entomología, Facultad de Recursos Naturales, Escuela Superior Politécnica de Chimborazo, Panamericana Sur Km 1.5, Riobamba, Ecuador.

[*] Corresponding author: santijaumes@hotmail.com; s.jaume@leibniz-lib.de
[2] Email: i.kilian@leibniz-lib.de
[3] Email: marabuntalex@gmail.com
[4] Email: x.mengual@leibniz-lib.de

[1] urn:lsid:zoobank.org:author:CB8722CA-9B1E-4BB6-AF0C-1A8BD57CC096
[2] urn:lsid:zoobank.org:author:B1ED76B4-2C0C-4621-9F46-F602954DDAC6
[3] urn:lsid:zoobank.org:author:3BA927BD-71D8-4917-8269-A987B30350D4
[4] urn:lsid:zoobank.org:author:A509310D-B567-4830-B8A4-BCB139BB8768

Abstract. In this study, we revise the genus *Bryopharsos* and describe nine new species. These include *B. curvum* Jaume-Schinkel sp. nov., *B. gorgona* Jaume-Schinkel sp. nov., and *B. tetracanthus* Jaume-Schinkel sp. nov. from Colombia; *B. insperatum* Jaume-Schinkel sp. nov. from Costa Rica; *B. asymmetricum* Jaume-Schinkel sp. nov. and *B. septenacula* Jaume-Schinkel sp. nov. from Ecuador; *B. bitenacula* Jaume-Schinkel sp. nov. and *B. chuspi* Jaume-Schinkel sp. nov. from Peru; and *B. bifidum* Jaume-Schinkel sp. nov. from Venezuela. Additionally, we report new geographical records of *B. amazonensis* Bravo & Araújo, 2019 from Colombia and Ecuador and new records of *B. clavigum* Quate, 1996, *B. claviformosum* Quate, 1996, and *B. palpiculum* Quate, 1996 from Ecuador. These new records correspond to the first report of *Bryopharsos* from Colombia, Ecuador, Peru, and Venezuela. Furthermore, we provide the first description of a *Bryopharsos* egg along with the redescription of the female of *B. palpiculum*. We also make available the first DNA barcodes for several species including *Bryopharsos asymmetricum*, *B. amazonensis*, *B. clavigum*, *B. claviformosum*, *B. palpiculum*, and *B. septenacula.* Lastly, we update the identification key to the known species, present a distribution map of the known taxa, and discuss the potential distribution of the genus in the Neotropical Region using a species distribution model.

Keywords. Integrative taxonomy, DNA barcoding, Neotropical Region, Psychodinae, new taxa, new record.

Jaume-Schinkel S., Kilian I.C., Pazmiño-Palomino A. & Mengual X. 2025. Revision of the genus *Bryopharsos* Quate, 1996 (Diptera: Psychodidae) with the description of nine new species. *European Journal of Taxonomy* 1001: 1–51. https://doi.org/10.5852/ejt.2025.1001.2951

Introduction

Bryopharsos is a small genus of Neotropical moth flies (Diptera Linnaeus, 1758: Psychodidae Newman, 1834) described by Quate (1996) to include four species from Costa Rica, namely *Bryopharsos claviformosum* Quate, 1996, *B. clavigum* Quate, 1996, *B. palpiculum* Quate, 1996, and *B. tritaleum* Quate, 1996. Posteriorly, Quate (1999) recorded *B. palpiculum* in Panama and described the female of that species, which remains the only known female of this genus.

Recently, Bravo & Araújo (2019) described three new *Bryopharsos* species from Brazil, namely *B. paulistensis* Bravo & Araújo, 2019, *B. uncinatum* Bravo & Araújo, 2019, and *B. amazonensis* Bravo & Araújo, 2019, bringing the total number of *Bryopharsos* species to seven and expanding the previously known distribution from Central America to South America.

Species within *Bryopharsos* are morphologically similar to species of the Oriental-Palearctic genus *Saximormia* Ježek, 1984 (Ježek 2010; Bravo & Araújo 2019), both genera can be identified in bulk samples containing Psychodidae specimens by their distinctively asymmetrical flagellomeres and the gonostyli being club-shaped with rounded apices. To date, the larval stages for the whole genus remain unknown, and nothing is known about their biology.

The aim of this study is to revise the genus *Bryopharsos* by presenting morphological and molecular evidence, and new geographical records for several species. We also aim to update the diagnosis of the genus and to provide an identification key for the known males for the world species.

Material and methods

Zoological collections

The examined material is deposited in different entomological collections referred to by their abbreviations in the text. The specimens processed at ZFMK were labeled with ZFMK-DIP and / or ZFMK-TIS numbers. These specimen-specific identifiers are also used to refer to the same specimens in the MECN collection in Ecuador, until permanent identifiers are assigned. The corresponding specimen data and identification numbers can be found in the BOLD dataset (see Molecular analyses below).

The abbreviations used for collections and their equivalents are given below:

INBio = Instituto Nacional de Biodiversidad, Heredia, Costa Rica
LACM = Natural History Museum of Los Angeles County, California, United States
MECN = Entomological Collection, Instituto Nacional de Biodiversidad, Quito, Ecuador
MZFS = Entomological Collection Prof. Johann Becker, Museu de Zoologia da Universidade Estadual de Feira de Santana, Bahia, Brazil
ZFMK = Museum Koenig, Leibniz-Institut zur Analyse des Biodiversitätswandels (previously known as Zoologisches Forschungsmuseum Alexander Koenig), Bonn, Germany

Molecular analyses

For 54 of the specimens deposited in ZFMK, we employed a non-destructive approach to analyze complete specimens. The process involved the utilization of a Qiagen (Hilden, Germany) BioSprint 96 magnetic bead extractor and the associated kits, following the guidelines provided by the manufacturer. To amplify

the 5'-end of the Cytochrome *c* Oxidase subunit I (COI) gene, the primers HCO2198-JJ (forward) and LCO1490-JJ (reverse) were utilized (Astrin & Stüben 2008). PCR amplification was carried out using a QIAGEN Multiplex PCR Kit and a TouchDown PCR (TD-PCR) method, as described by Korbie & Mattick (2008). Subsequently, the PCR products were sent to the Beijing Genomic Institute (BGI) in Hong Kong, China, for bidirectional sequencing. The obtained DNA sequences were then assembled, aligned, and cleaned using Geneious Prime ver. 2022.1.1 (Biomatters, Auckland, New Zealand). The final sequence length was 658 bp.

Geneious Prime ver. 2022.1.1 (Biomatters, Auckland, New Zealand) was used to conduct a distance-based neighbor-joining (NJ) analysis (Saitou & Nei 1987) using the Jukes-Cantor model. For the NJ tree, we constrained the COI sequence of *Alepia viatrix* Jaume-Schinkel, Kvifte, Weele & Mengual, 2022, (GenBank accession number: OK345511) as the root to help with the visualization. The sequences used in the analysis, specimen metadata including collection numbers for specimens processed at ZFMK and GenBank accession numbers can be accessed on BOLD under the dataset DS-BRYO (available at: https://doi.org/10.5883/DS-BRYO). Bootstrap support (BS) values were estimated through 1000 replicates generated in Geneious.

Species records

A map was generated to visualize the distribution of the species of *Bryopharsos* based on the geographic coordinates extracted from the localities reported in the literature. For those records without exact reported coordinates we looked for the reported locality and adjusted the coordinates using Google® Earth. As some species have overlap in their distribution we used the Rstudio (ver. 2023.03.1+446) package 'ggplot', with the 'geom_jitter' and 'theme_bw' functions to enhance the visualization and apply a black-and-white theme to the map. This approach facilitated the visualization of the spatial distribution of *Bryopharsos* when species distribution overlap.

Genus distribution model

The genus distribution model was built using the software MaxEnt ver. 3.4.4 (Phillips *et al.* 2023) using species geographical records to model the potential distribution of the genus. Since the known species are restricted to the Neotropical Region, the resulting map was trimmed to the American continent. Climate variables were obtained from WorldClim (Fick & Hijmans 2017).

Terminology

We follow the general terminology proposed by Cumming & Wood (2017) and Kvifte & Wagner (2017a). For the reasons mentioned in the discussion, we use the term 'surstyli' to refer to the caudal appendages, which are also referred to as cercopods, surstyli, or hypopods (also see the discussion in Kvifte & Wagner 2017b).

Within the male terminalia of *Bryopharsos* species, there is a structure located on the gonocoxal lobes that resembles a spine-like projection. This structure is called appendage by Quate (1996), and Bravo & Araujo (2019) refer to it in the description of *B. paulistensis* as "lateral lobes projected posteriorly in the posterior expansion of the gonocoxal apodemes". We herein refer to it as the spine of the gonocoxal lobes (see Fig. 3).

In Psychodidae, the terminalia is inverted due to the rotation of segment nine, placing the epandrium (tergite 9) ventrally and the hypandrium (sternite 9) dorsally, with respect to the rest of the abdomen. For consistency, we consider the hypandrium as the ventral-most surface and the epandrium as the dorsal-most, as if the rotation never occurred. In this context, 'ventral' refers to or towards the hypandrium, and 'dorsal' to or towards the epandrium.

Results

Taxonomic account

Class Insecta Linnaeus, 1758
Order Diptera Linnaeus, 1758
Suborder Psychodomorpha Hennig, 1968
Family Psychodidae Newman, 1834
Subfamily Psychodinae Newman, 1834

Genus ***Bryopharsos*** Quate, 1996

Bryopharsos Quate, 1996: 40. Type species: *Bryopharsos palpiculum* Quate, 1996 by original designation.

Bryopharsos – Quate 1999: 434 (female description and updated distribution). — Ježek 2010: 237 (discussion of characters). — Kvifte 2018: 603 (tribal classification). — Bravo & Araújo 2019: 364 (description of new species and key to world species).

Species distribution shown in Fig. 1.

Diagnosis

Building upon Quate's (1996) original diagnosis, Bravo & Araújo (2019) proposed a broader diagnosis to accommodate their new Brazilian species. In this study, we update the genus diagnosis, including previously and herein described species. Male: vertex short, up to twice as wide as eye bridge; eye bridge contiguous conformed by 3–5 facet rows; antennae with 14 flagellomeres, 1–13 asymmetrically-nodiform, flagellomere 14 with long, digitiform apiculus; flagellomeres 1–13 with a pair of broad, leaf-shaped ascoids; ascoids width at least the same as the length of the flagellomere carrying them; palpi short reaching the level of the third flagellomere; labellum short and not bulbous; thorax with or without allurement organs; wing membrane with alveoli between longitudinal veins; wing vein R_5 ends at wing apex; gonocoxal apodemes fused or contiguous at midline; gonocoxal lobes projected anteriorly, with or without a spine; gonostyli digitiform to club-shaped with rounded apex; surstyli with 1–7 tenacula; aedeagal complex asymmetrical; ejaculatory apodeme width is equal to or greater than half of its total length in ventral view.

Bryopharsos was considered by Ježek (2010) to be morphologically close to the Palearctic/Oriental genus *Saximormia* as they share the following characters: ascoids as broad as or broader than the flagellomere carrying them, eyes contiguous in the eye bridge, and the general wing structure of the wing. Nevertheless, they can be easily differentiated from each other by the following characters: alveoli on the wing membrane present in *Bryopharsos* (absent in *Saximormia*), wing vein radial and medial forks being at the same level and basal to the wing center in *Bryopharsos* (forks not being at the same level and apical to the wing center in *Saximormia*), vein R_5 ending at wing apex in *Bryopharsos* (vein R_5 ending at wing margin posterior to the apex in *Saximormia*), the ejaculatory apodeme is conspicuously enlarged in ventral view in *Bryopharsos* (ejaculatory apodeme not enlarged in *Saximormia*), gonostyli club-shaped with a rounded blunt apex in *Bryopharsos* (gonostyli tapering towards the apex and with a pointed apex in *Saximormia*) (Ježek 2010; Bravo & Araújo 2019).

Bryopharsos amazonensis Bravo & Araújo, 2019
Figs 1–3

Bryopharsos amazonensis Bravo & Araújo, 2019: 368. Type locality: Brazil, 15 km SE of Rio Branco, EMBRAPA (holotype male, MZFS).

Diagnosis

Male

Eye bridge with four facet rows (Fig. 2A); wing 1.8 times as long as wide (Fig. 2B); ejaculatory apodeme paddle-shaped in ventral view; surstyli with five tenacula of equal length; aedeagus long, triangular, and with a pointed apex (Figs 2C, 3A–B). According to Bravo & Araújo (2019), *B. amazonensis* is morphologically similar to *B. clavigum* and *B. claviformosum*, but it can be differentiated by the number of tenacula (four in *B. clavigum*; five in *B. amazonensis* and *B. claviformosum*) and the length of the tenacula (four long and one short in *B. claviformosum* (Fig. 3C–D), five of equal length in *B. amazonensis*; four of the same length in *B. clavigum*).

Female

Unknown.

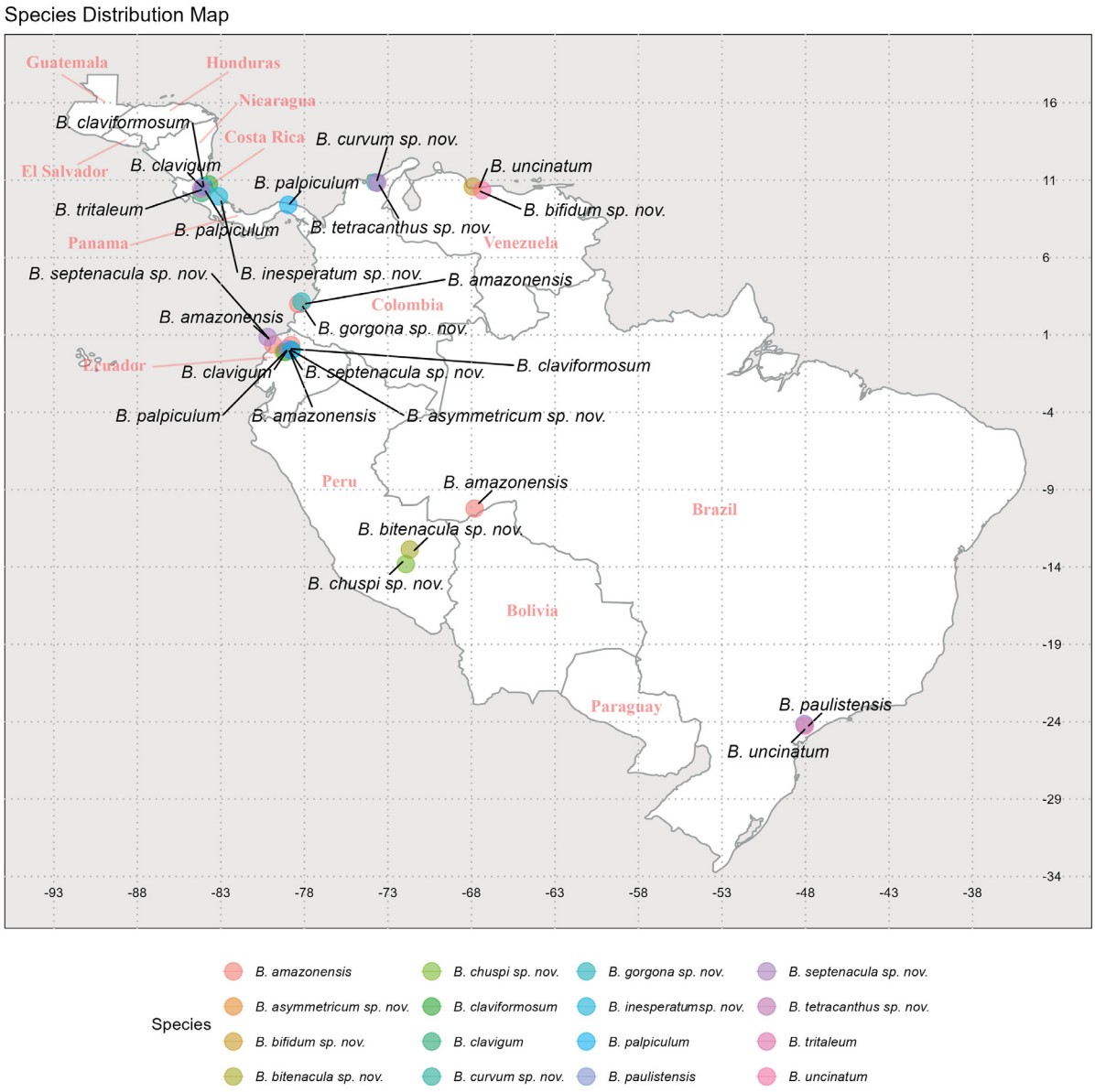

Fig. 1. Species distribution map. Species dots do not represent the actual localities; jitter was added for visualization as the species' real distributions overlap.

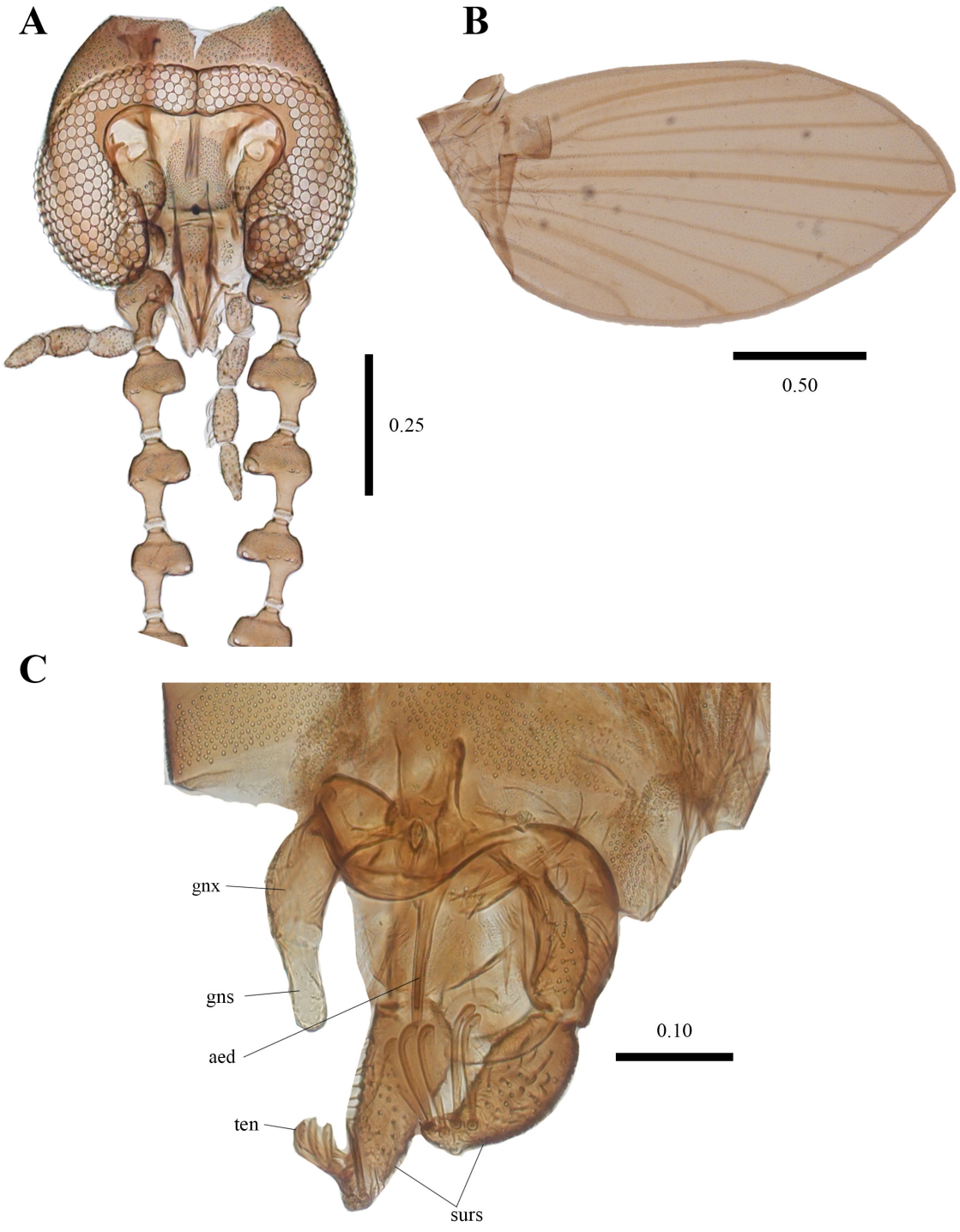

Fig. 2. *Bryopharsos amazonensis* Bravo & Araújo, 2019, ♂ (ZFMK-TIS-2628286). **A**. Head. **B**. Wing. **C**. Terminalia (ventral view). Abbreviations: aed = aedeagus; gns = gonostylus; gnx = gonocoxite; surs = surstyli; ten = tenacula. All scale bars are in millimeters.

Material examined

ECUADOR – **Pichincha** • 9 ♂♂; Pedro Vicente Maldonado, Parroquia Pedro Vicente Maldonado, near San Pancracio, roadway to Pachijal; 0.11862° N, 78.95802° E; alt. 750 m; 25–28 Jan. 2022; Isabel Kilian leg.; ZFMK, ZFMK-TIS-2628286, ZFMK-TIS-2628287, ZFMK-TIS-2628288, ZFMK-TIS-2628289, ZFMK-TIS-2628298, ZFMK-TIS-2628299, ZFMK-TIS-2628303, ZFMK-TIS-2628304, ZFMK-TIS-2628307 • 2 ♂♂; same data as for preceding; 0.11561° N, 78.95805° E; 1–9 Feb. 2022; ZFMK, ZFMK-TIS-2636932, ZFMK-TIS-2636935 • 6 ♂♂; same data as for preceding; MECN, ZFMK-TIS-2636989, ZFMK-TIS-2637097, ZFMK-TIS-2637102, ZFMK-TIS-2637110, ZFMK-TIS-2637122, ZFMK-TIS-2637145 • 8 ♂♂; same data as for preceding; MECN, ZFMK-TIS-2637067, ZFMK-TIS-2637069, ZFMK-TIS-2627070, ZFMK-TIS-2627072, ZFMK-TIS-2627074, ZFMK-TIS-2627075, ZFMK-TIS-2627076, ZFMK-TIS-2627078.

COLOMBIA – **Cauca** • 5 ♂♂ Guapí, Gorgona Island, alta El Mirador; alt. 180 m; 4–24 Mar. 2000; R. Doque leg.; LACM, LACM ENT 279390, LACM ENT 279391, LACM ENT 279392, LACM ENT 279399, LACM ENT 279398.

Distribution

Brazil (Bravo & Araújo 2019), Colombia (this publication, new record), and Ecuador (this publication, new record) (Fig. 1).

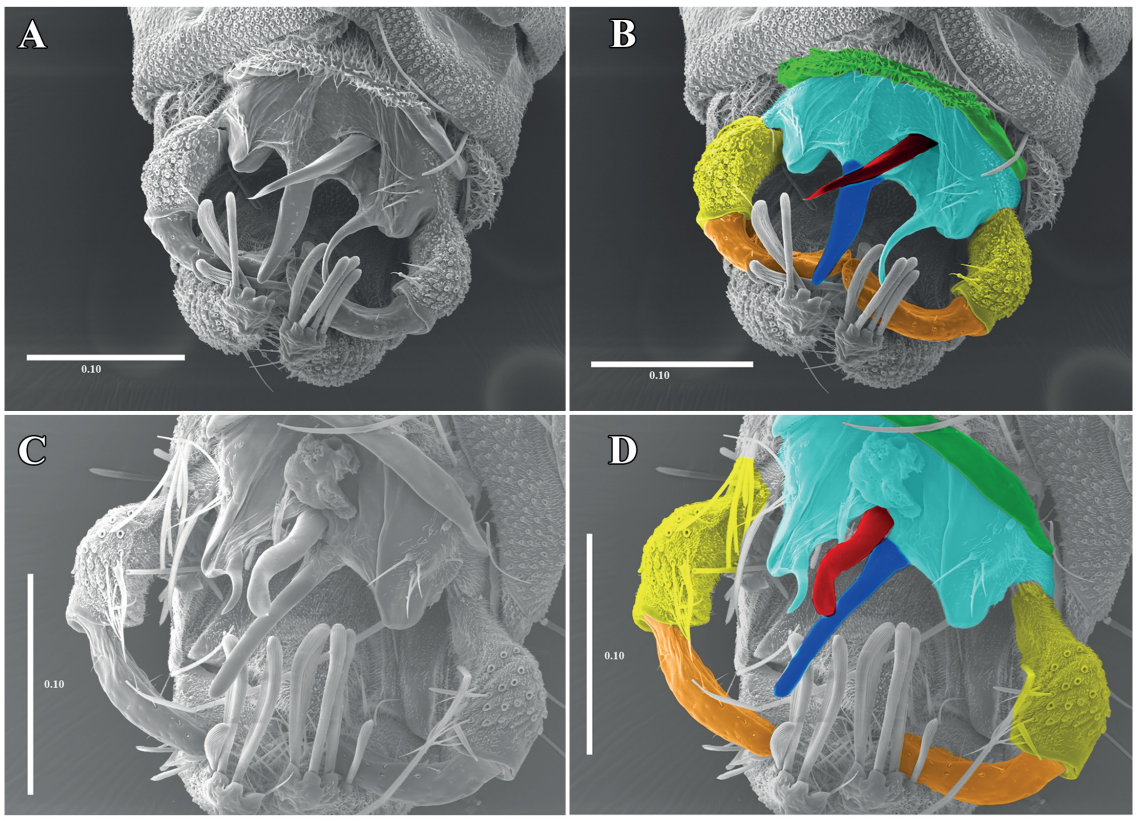

Fig. 3. SEM pictures of male terminalia (ventral view). **A–B**. *Bryopharsos amazonensis* Bravo & Araújo, 2019. **C–D**. *Bryopharsos claviformosum* Quate, 1996. Colors: blue = paramere; cyan = gonocoxal lobes; green = hypandrium; orange = gonostyli; red = aedeagus; yellow = gonocoxites. All scale bars are in millimeters.

DNA barcodes

22 specimens were successfully sequenced: ZFMK-TIS-2628286, ZFMK-TIS-2628288, ZFMK-TIS-2628289, ZFMK-TIS-2628298, ZFMK-TIS-2628303, ZFMK-TIS-2628304, ZFMK-TIS-2628307, ZFMK-TIS-2636932, ZFMK-TIS-2636935, ZFMK-TIS-2636989, ZFMK-TIS-2637067, ZFMK-TIS-2637069, ZFMK-TIS-2627070, ZFMK-TIS-2627072, ZFMK-TIS-2627074, ZFMK-TIS-2627075, ZFMK-TIS-2627076, ZFMK-TIS-2627078, ZFMK-TIS-2637097, ZFMK-TIS-2637102, ZFMK-TIS-2637110, ZFMK-TIS-2637122. The maximum intraspecific uncorrected pairwise distance for COI sequences was 0.37% or 3 bp.

Remarks

Three specimens (ZFMK-TIS-2636935, ZFMK-TIS-2636989, ZMFK-TIS-2637097) have a small morphological variation as they present a spine in the gonocoxal apodeme, while the remaining specimens do not present the spine. The molecular evidence and the remaining morphological characters suggest all specimens belong to the same species. The original differentiation of *B. amazonensis* and *B. claviformosum* by Bravo & Araújo (2019) based on the difference in tenacula lengths (five of the same length in *B. amazonensis*; four of equal length and one shorter in *B. claviformosum*) appears to be a good morphological character to separate them. This is further supported by molecular data in this study.

Bryopharsos asymmetricum Jaume-Schinkel sp. nov.
urn:lsid:zoobank.org:act:40B57D7B-F290-4EF5-A80D-D7E78C86F1EC
Figs 1, 4–5

Diagnosis

Male

Eye bridge with five facet rows (Fig. 4A); wing 2.2 times as long as wide; ejaculatory apodeme convex in ventral view; gonocoxal apodeme with spine projection; surstyli with 2 or 3 tenacula; aedeagus digitiform and evenly tapering towards apex (Fig. 4C). This species is similar to *B. tritaleum*, but they can be differentiated by the number of tenacula (three in *B. tritaleum*, some specimens with three tenacula on one surstylus in *B. asymmetricum* sp. nov. but the remaining with two tenacula), the number of facet rows in the eye bridge (four in *B. tritaleum*, five in *B. asymmetricum*), and the length of the ejaculatory apodeme (about as long as the aedeagus in *B. tritaleum*, shorter than the aedeagus in *B. asymmetricum*).

Female

Unknown.

Etymology

The specific name '*asymmetricum*' derives from the Greek word 'συμμετρικός' (symetrikós) with the Greek prefix 'ἀ-' (without), and it referrs to the asymmetrical number of apical tenacula on the surstyli. Specific name to be treated as an adjective.

Type material

Holotype

ECUADOR – **Pichincha** • ♂; Pedro Vicente Maldonado, Parroquia Pedro Vicente Maldonado, near San Pancracio, roadway to Pachijal; 0.11561° N, 78.95805° E; alt. 750 m; 1–9 Feb. 2022; Isabel Kilian leg.; MECN, ZFMK-TIS-2637130.

Paratypes

ECUADOR – **Pichincha** • 9 ♂♂; same data as for holotype; ZFMK, ZFMK-TIS-2629868, ZFMK-TIS-2629902, ZFMK-TIS-2636934, ZFMK-TIS-2637062, ZFMK-TIS-2637064, ZFMK-TIS-2637068,

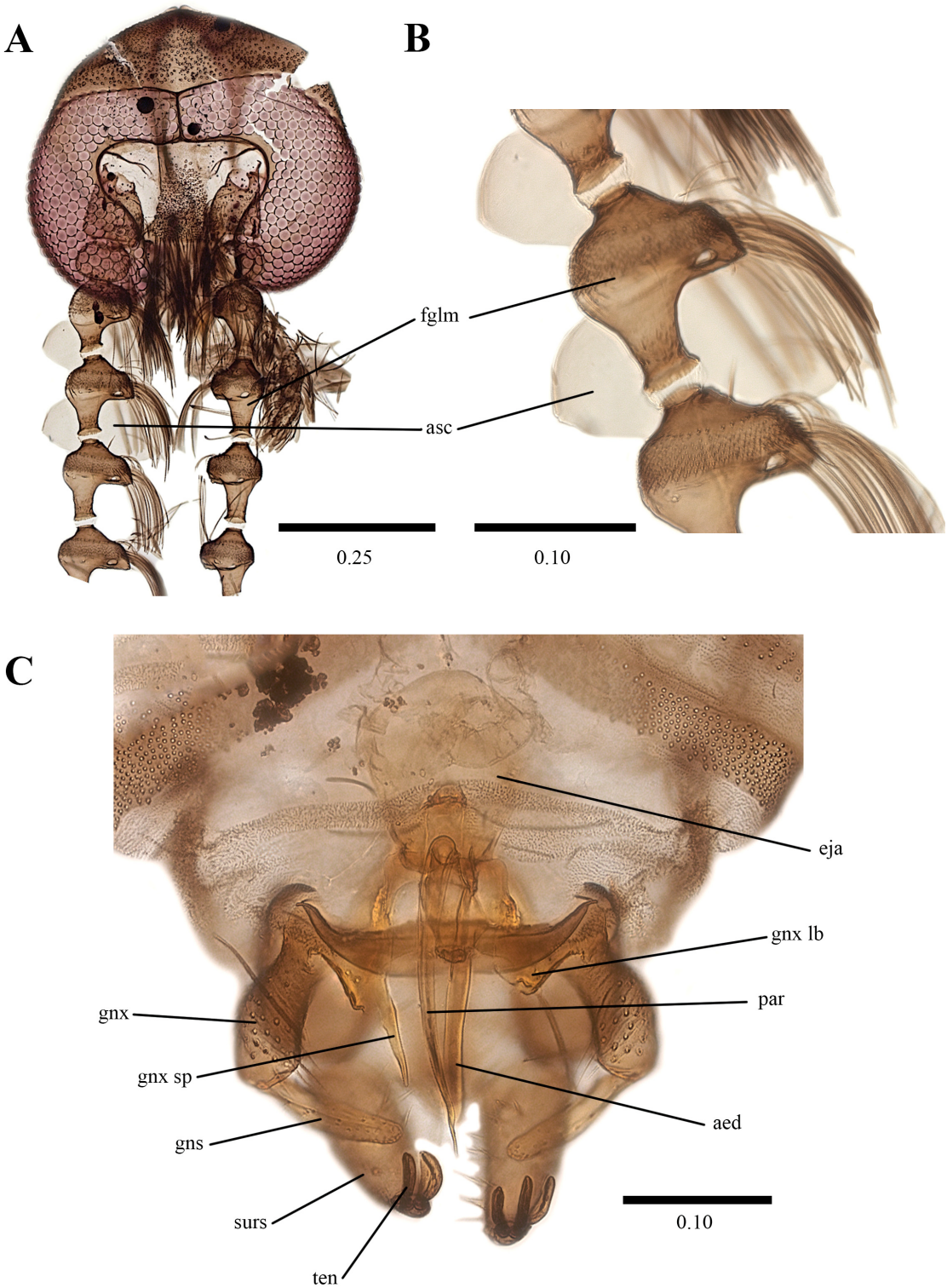

Fig. 4. *Bryopharsos asymmetricum* Jaume-Schinkel sp. nov., holotype, ♂ (MECN, ZFMK-TIS-2637130). **A**. Head. **B**. Antennal segments. **C**. Terminalia (ventral view). Abbreviations: aed = aedeagus; asc = ascoids; eja = ejaculatory apodeme; fglm = flagellomere; gns = gonostylus; gnx = gonocoxite; gnx lb = gonocoxal lobes; gnx sp = spine of the gonocoxal lobes; par = paramere; surs = surstyli; ten = tenacula. All scale bars are in millimeters.

ZFMK-TIS-2637077, ZFMK-TIS-2637115, ZFMK-TIS-2637127 • 1 ♂; same data as for holotype; MECN, ZFMK-TIS-2637149.

Description

Measurements. In mm (n = 6). Wing length: 1.90 (1.95–1.80), wing width: 0.85 (0.90–0.80); head length: 0.50 (0.50–0.45), head width: 0.40 (0.47–0.38); antennal segments (Fig. 4B): scape: 0.11 (0.11–0.10), pedicel: 0.06 (0.06–0.05), flagellomeres 1–5: 0.1 (0.12–0.11); palpal segment 1: 0.05 (0.5–0.05), palpal segment 2: 0.07 (0.08–0.06), palpal segment 3: 0.07 (0.08–0.07), palpal segment 4: 0.08 (0.08–0.07).

Holotype male

Head (Fig. 4A). Slightly longer than wide; eye bridge contiguous with five rows of facets, interocular suture absent (Fig. 4A); post-ocular alveoli not enlarged and non-distinguishable from the remaining alveoli on the head; the frontal patch of alveoli not divided, upper margin with a concavity in the middle, lower margin rounded. Antennal scape about two times as long as pedicel, almost cylindrical; pedicel spherical, smaller than scape; flagellomeres asymmetrical and nodiform, with scattered setae on the basal half surface, apical flagellomeres absent in examined material, the maximum number of flagellomeres present five; ascoids rectangular and broad, about the same length, and about two times as wide as flagellomere carrying them. Palpal segments cylindrical, palpal segment 4 with pointed apex, palpal proportions: 1.0:1.5:1.5:1.6; labium without any strong sclerite; labella bulbous with seven three setae on outer margin and two setae on inner margin.

Thorax. Without allurement organs; all coxae with a stripe of three to five rows of alveoli. Wing length about 2.2 times its width; wing membrane brown-hyaline; alveoli distributed uniformly on wing membrane; subcostal vein short ending beyond the origin of R_4; fork of R_{2+3} at the same level as M_{1+2} and joining R_4; fork of M_{1+2} weak; R_5 ending at the wing apex; CuA_2 ending at wing margin.

Terminalia (Figs 4C, 5). Hypandrium is a distinct band that connects the gonocoxites, broad and plate-like; gonocoxites about the same length as gonostyli, gonostyli slightly incurved, with rounded-blunt apex; aedeagus digitiform, apex rounded, with an additional digitiform paramere, paramere evenly narrowing towards the apex, longer than aedeagus; ejaculatory apodeme shorter than aedeagus, basal margin convex; gonocoxal apodemes projected anteriorly as a trapezoidal plate, fused; epandrium narrow, about three times wider than long, with posterior margin concave; hypoproct tongue-shaped, longer than epandrium and covered in small setulae, epiproct shorter than hypoproct; surstyli evenly tapering towards the apex and curved, one with three apical tenacula, the other with two tenacula, tenacula with rounded apex.

Distribution

Only known from the type locality in Ecuador (Fig. 1).

DNA barcodes

Eleven specimens were successfully sequenced: ZFMK-TIS-2629868, ZFMK-TIS-2629902, ZFMK-TIS-2636934, ZFMK-TIS-2637062, ZFMK-TIS-2637064, ZFMK-TIS-2637068, ZFMK-TIS-2637077, ZFMK-TIS-2637115, ZFMK-TIS-2637127, ZFMK-TIS-2637130, ZFMK-TIS-2637149. All eleven obtained sequences are identical.

Remarks

The holotype and paragypes ZFMK-TIS-2629868, ZFMK-TIS-2637115, and ZFMK-TIS-2637149 have three tenacula in one surstylus and two in the other, while the paratypes ZFMK-TIS-2629902 and ZFMK-TIS-2637127 only present two tenacula on both surstyli (no empty alveoli for a missing tenaculum is distinguishable), which leads us to believe this character is variable. The presence of one tenaculum in one surstylus and two on the other has also been recorded in the holotype of *B. paulistensis* (Bravo &

Araujo 2019: fig. 24). Furthermore, the spine in the gonocoxal apodeme is present either on the right side or on the left side, which is also a variable character inside the examined material. Nonetheless, the COI sequence of all specimens is identical, supporting our hypothesis that all the specimens belong to the same species.

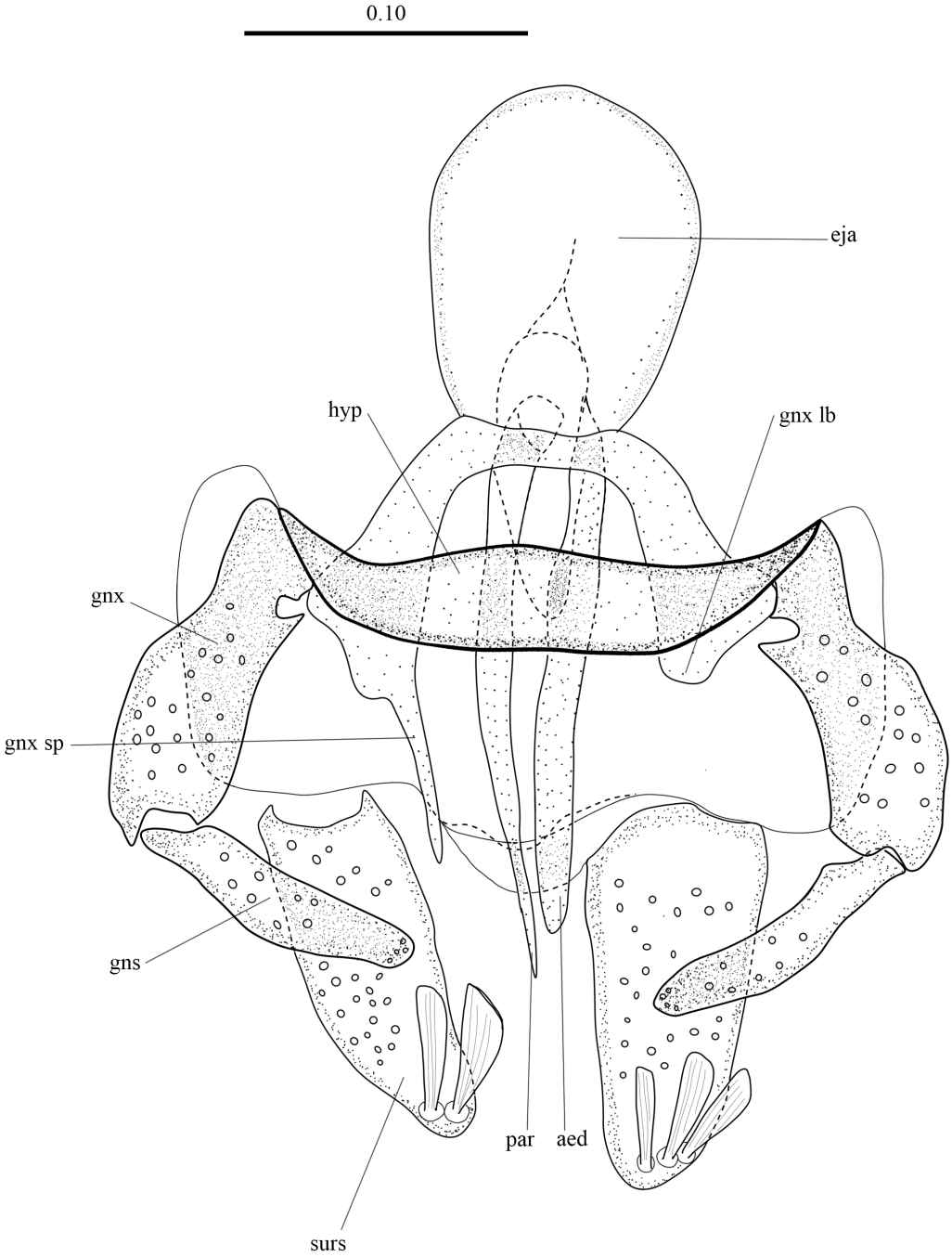

Fig. 5. *Bryopharsos asymmetricum* Jaume-Schinkel sp. nov., holotype, ♂ (MECN, ZFMK-TIS-2637130); terminalia (ventral view). Abbreviations: aed = aedeagus; eja = ejaculatory apodeme; gns = gonostylus; gnx = gonocoxite; gnx lb = gonocoxal lobes; gnx sp = spine of the gonocoxal lobes; hyp = hypandrium; par = paramere; surs = surstyli. Scale bar in millimeters.

Bryopharsos bifidum Jaume-Schinkel sp. nov.
urn:lsid:zoobank.org:act:E3E364DD-E83D-4ADB-8A1F-CAB198C11DF1
Figs 1, 6–7

Diagnosis

Male

Eye bridge with three facet rows (Fig. 6A); wing 1.9 times as long as wide; ejaculatory apodeme ovoid, with anterior margin straight, slightly longer than the aedeagus; gonocoxal apodeme fused; surstyli with a single apical tenaculum; aedeagus digitiform, curved, with rounded apex. This species shares the same number of apical tenacula in the surstyli but it can be easily differentiated by having bifurcated gonostyli (no other known *Bryopharsos* species has bifurcated gonostyli).

Female

Unknown.

Etymology

The specific name '*bifidum*' derives from Latin '*bifidus*' meaning split into two parts, referring to the bifurcate gonostyli. Name to be treated as a noun in apposition.

Type material

Holotype

VENEZUELA – **Aragua** • ♂; 19 km N of Maracay; 14–17 Oct. 1993; alt. 1280 m; L.W. Quate leg.; Malaise trap; Mounted in Euparal; LACM, LACM-ENT-279295.

Paratype

VENEZUELA – **Choroní** • 1 ♂; 22 km S of Choroní; 17 Oct. 1993; alt. 1000 m.; L.W. Quate leg.; Malaise Trap; Mounted in Euparal; LACM, LACM-ENT-279294.

Description

Measurements. In mm (n = 2). Wing length: 2.34 (2.24–2.45), wing width: 1.19 (1.17–1.22); head length: 0.60 (0.60–0.60), head width: 0.79 (0.71–0.86); antennal segments: scape: 0.10 (0.10–0.10), pedicel: 0.08 (0.07–0.08), flagellomere 1: 0.14 (0.13–0.14), flagellomeres 2–12: 0.15 (0.14–0.15), flagellomere 13: 0.06 (0.06–0.06), flagellomere 14: 0.08 (0.08–0.08); palpal segment 1: 0.05 (0.05–0,05), palpal segment 2: 0.05 (0.05–0.05), palpal segment 3: 0.05 (0.05–0.05), palpal segment 4: 0.04 (0.04–0.04).

Holotype male

Head (Fig. 6A). A little wider than long; eye bridge contiguous, with three rows of facets, interocular suture absent; post-ocular alveoli not enlarged and non-distinguishable from the remaining alveoli on the head; frontal patch of alveoli not divided, triangular with the lower margin rounded. Antennal scape slightly longer the length of the pedicel, cylindrical; pedicel spherical; 14 flagellomeres asymmetrical and nodiform, with scattered setae on the basal half surface, apical flagellomere with terminal apiculus; ascoids absent in examined material. Palpal segments cylindrical, palpal segment 4 apically pointed, palpal proportions: 1.0:1.0:1.0:0.8; labium without any strong sclerite; labella not bulbous with 3–4 setae on outer margin.

Thorax. Without allurement organs; all coxae with a stripe of three to five rows of alveoli. Wing length about 2.1 times its width; wing membrane brown-hyaline; alveoli distributed uniformly on wing membrane; subcostal vein short ending beyond the origin of R_4; fork of R_{2+3} basal to the level of M_{1+2} and joining R_4; fork of M_{1+2} weakly sclerotized; R_5 ending at the wing apex; CuA_2 ending at wing margin.

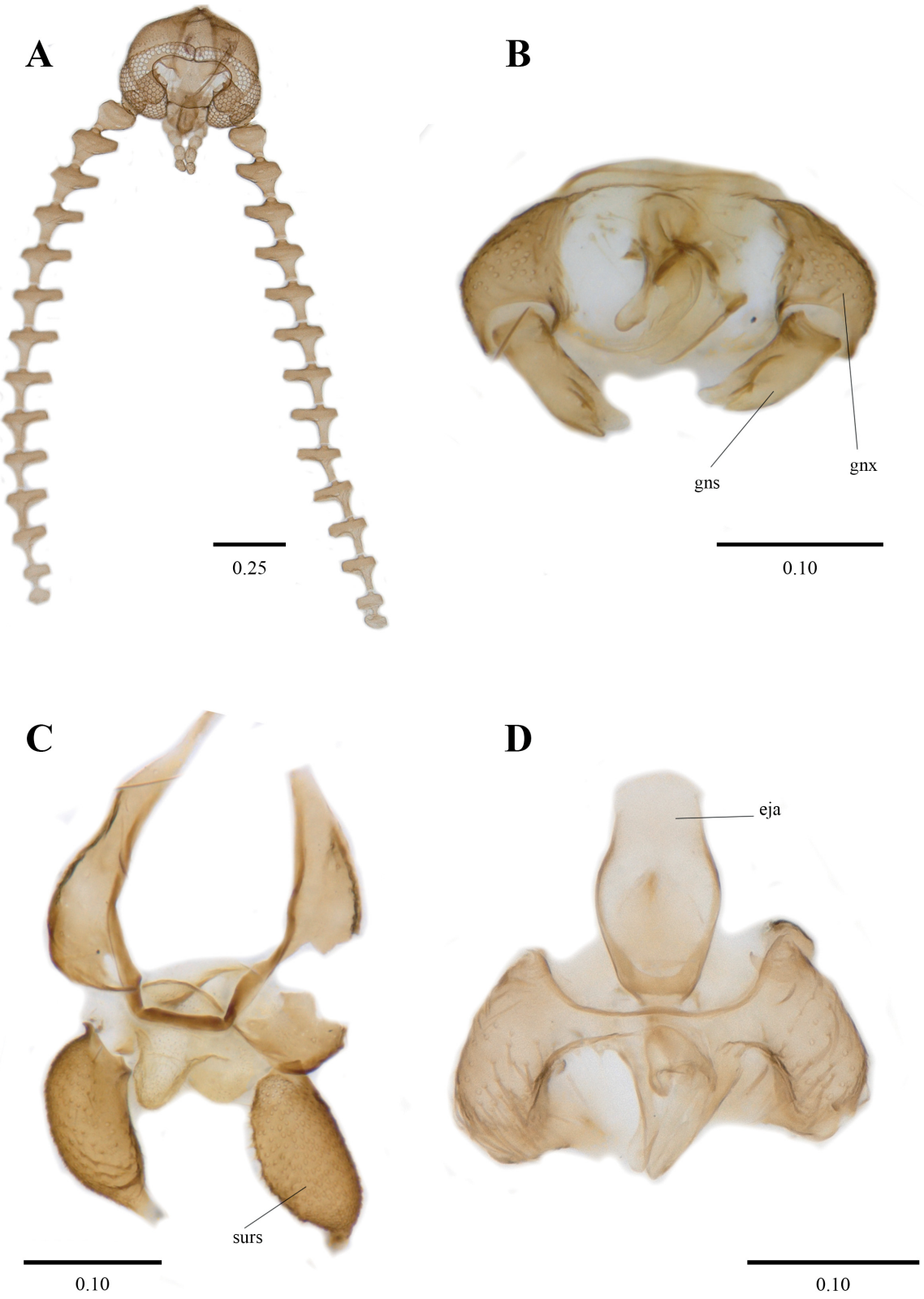

Fig. 6. *Bryopharsos bifidum* Jaume-Schinkel sp. nov., holotype, ♂ (LACM-ENT-279294). **A**. Head. **B**. Terminalia. **C**. Surstyli. **D**. Terminalia. Abbreviations: eja = ejaculatory apodeme; gns = gonostylus; gnx = gonocoxite; surs = surstyli. All scale bars are in millimeters.

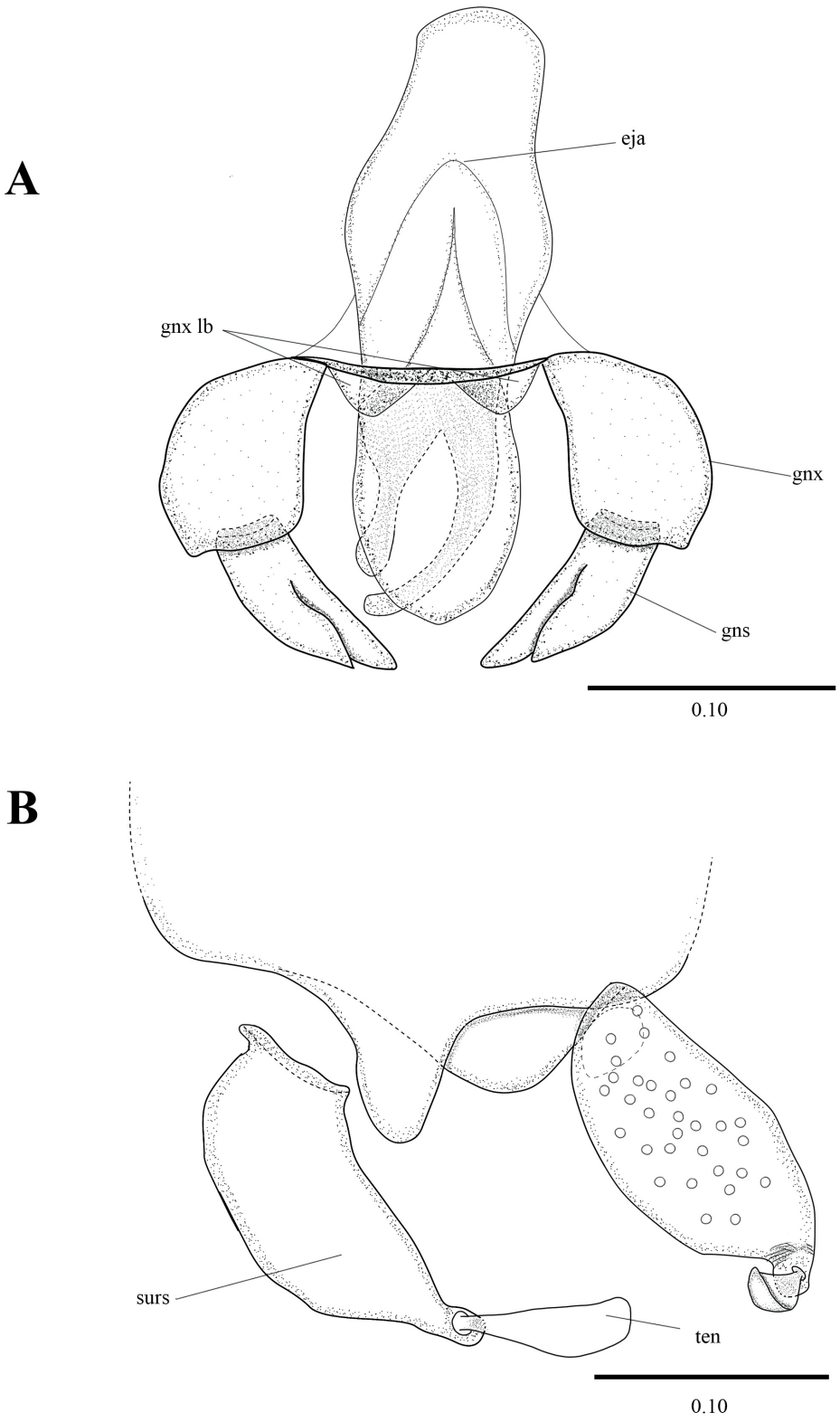

Fig. 7. *Bryopharsos bifidum* Jaume-Schinkel sp. nov., holotype, ♂ (LACM-ENT-279294). **A**. Terminalia (ventral view). **B**. Surstyli (ventral view). Abbreviations: eja = ejaculatory apodeme; gns = gonostylus; gnx = gonocoxite; gnx lb = gonocoxal lobes; surs = surstyli; ten = tenacula. All scale bars are in millimeters.

Terminalia (Figs 6B–D, 7). Hypandrium is a distinct band that connects the gonocoxites, plate-like; gonocoxites cylindrical, about the same length as gonostyli; gonostyli bifurcated, bifurcation occurs around half, both rami have rounded apex, mesal ramus digitiform, lateral ramus ovate; gonocoxal apodeme without anterior projections; gonocoxal lobes with six setae on each side; aedeagus digitiform, curved, apex rounded, ending beyond the apex of the paramere, paramere digitiform, almost thumb-like, with rounded apex; ejaculatory apodeme with rounded margin, about the same length as the aedeagus; epandrium plate-like, about two times as wide as long; hypoproct tongue-shaped, and covered in small setulae, epiproct broader and shorter than hypoproct; surstyli conical, abruptly narrowing towards the apex, curved ventrally, with a single apical tenaculum, tenaculum with rounded apex.

Distribution

Only known from the type locality in Venezuela (Fig. 1).

DNA barcodes

No specimens were available for DNA extraction.

Remarks

Both specimens presented a label with L.W. Quate's handwriting reading "*Bryopharsos bifidum*", this specific name was never published nor was the description of the species, so we decided to keep the name chosen by Quate as it is fitting for the species.

Bryopharsos bitenacula Jaume-Schinkel sp. nov.
urn:lsid:zoobank.org:act:D6D6DE95-B8A7-430B-B4B0-AD99DA55F54F
Figs 1, 8–9

Diagnosis

Male

Eye bridge with three facet rows (Fig. 8A); wing 2.1 times as long as wide; ejaculatory apodeme ovoid, with anterior margin straight, shorter than the aedeagus; gonocoxal apodeme projecting anteriorly; surstyli with two apical tenacula; aedeagus digitiform, with rounded apex, paramere digitiform and longer than aedeagus. This species shares the same number of apical tenacula in the surstyli as *B. asymmetricum* sp. nov. but it can be easily differentiated by the shape of the paramere (digitiform with pointed apex in *B. asymmetricum*, digitiform and with rounded apex in *B. bitenacula* sp. nov.), and the length of the paramere (shorter than the aedeagus in *B. bitenacula*, longer than the aedeagus in *B. asymmetricum*).

Female

Unknown.

Etymology

The specific name derives from the Latin word '*bi*' meaning two, and '*tenacula*'. It makes reference to the two apical tenacula present in the surstyli. To be treated as a noun in apposition.

Type material

Holotype

PERU – **Cuzco** • ♂; 26 km West of Pilcopata; 13.055° N, 71.546667° E; alt. 1500 m; 24 Jul.–2 Aug. 1997; L.W. Quate leg.; Malaise trap; Cloud Forest; Mounted in Euparal; LACM, LACM-ENT-279272.

Paratypes

PERU – **Cuzco** • 12 ♂♂; same data as for holotype; LACM, LACM-ENT-279266, LACM-ENT-279267, LACM-ENT-279268, LACM-ENT-279269, LACM-ENT-279270, LACM-ENT-279273, LACM-

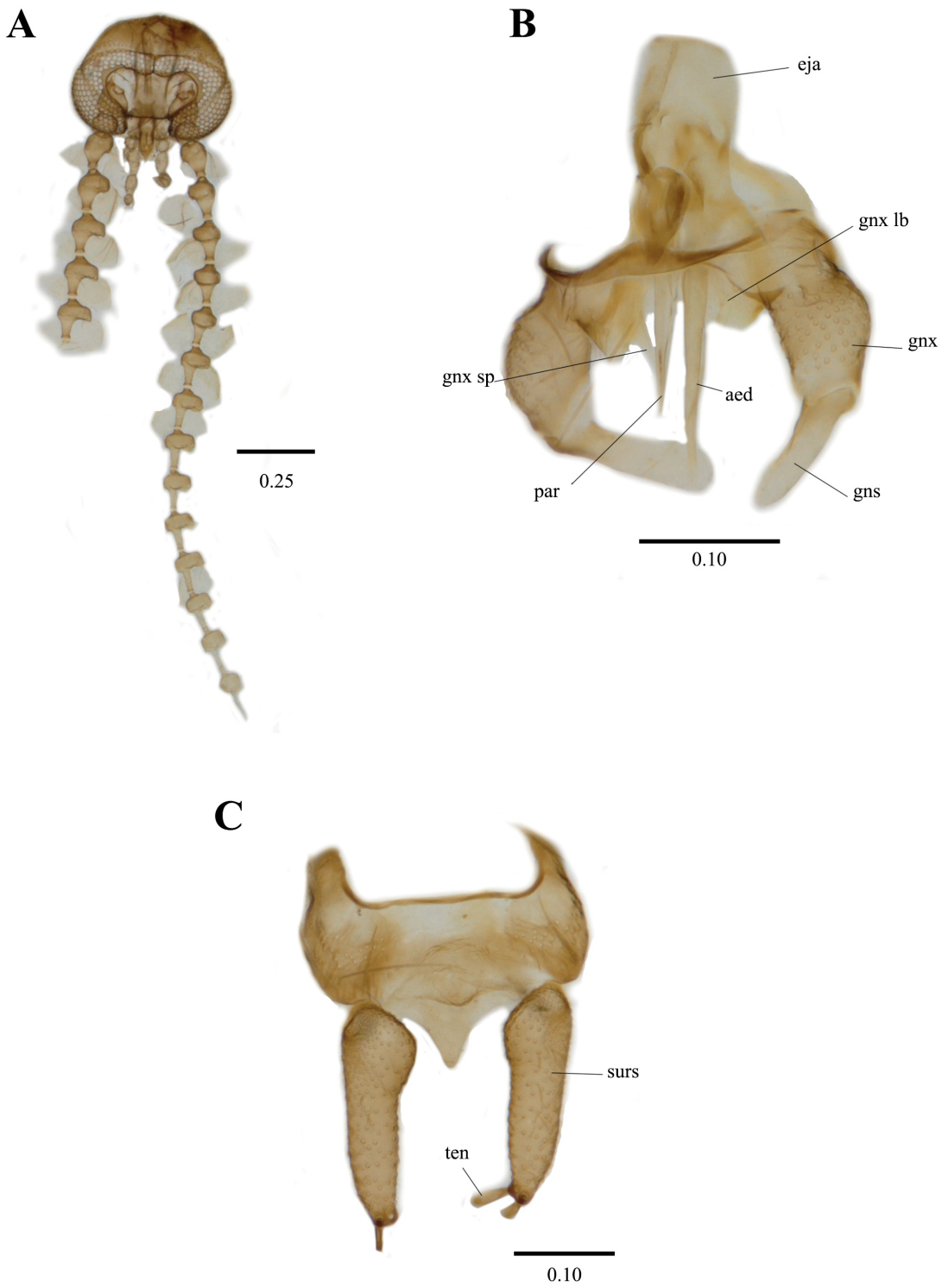

Fig. 8. *Bryopharsos bitenacula* Jaume-Schinkel sp. nov., holotype, ♂ (LACM-ENT-279272). **A**. Head. **B**. Terminalia. **C**. Surstyli. Abbreviations: aed = aedeagus; eja = ejaculatory apodeme; gns = gonostylus; gnx = gonocoxite; gnx lb = gonocoxal lobes; gnx sp = spine of the gonocoxal lobes; par = paramere; surs = surstyli; ten = tenacula. All scale bars are in millimeters.

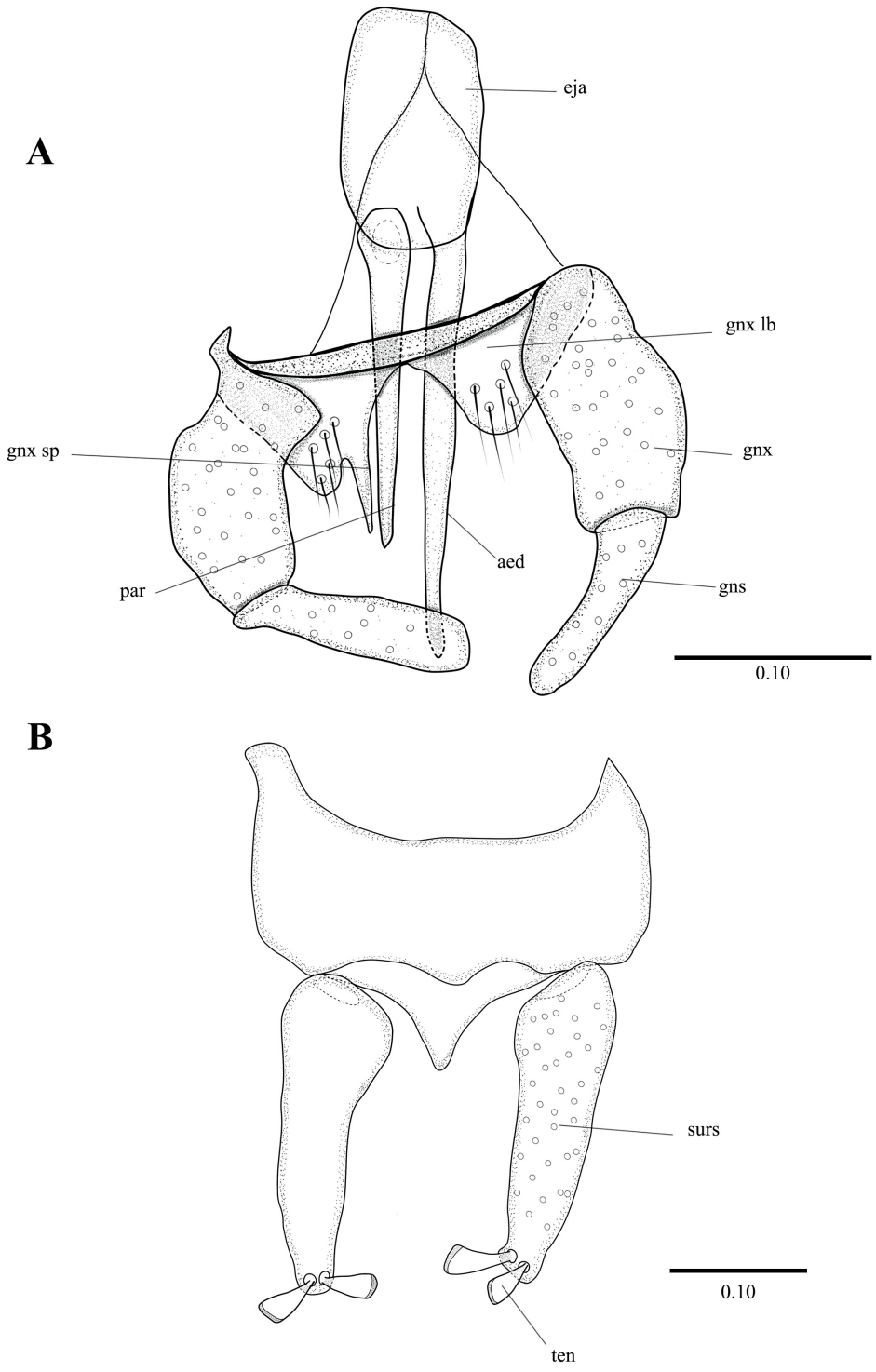

Fig. 9. *Bryopharsos bitenacula* Jaume-Schinkel sp. nov., holotype, ♂ (LACM-ENT-279272). **A**. Terminalia (ventral view). **B**. Surstyli (ventral view). Abbreviations: aed = aedeagus; eja = ejaculatory apodeme; gns = gonostylus; gnx = gonocoxite; gnx lb = gonocoxal lobes; gnx sp = spine of the gonocoxal lobes; par = paramere; surs = surstyli; ten = tenacula. All scale bars are in millimeters.

ENT-279274, LACM-ENT-279275, LACM-ENT-279277, LACM-ENT-279278, LACM-ENT-279290, LACM-ENT-279291 • 1 ♂, same data as for holotype; 25 Jul.–3 Aug. 1997; LACM, LACM-ENT-279381.

Description

Measurements. In mm (n = 8). Wing length: 2.38 (2.24–2.45), wing width: 1.23 (1.17–1.22); head length: 0.43 (0.42–0.50), head width: 0.54 (0.52–0.68); antennal segments: scape: 0.10 (0.10–0.10), pedicel: 0.08 (0.07–0.08), flagellomere 1: 0.12 (0.12–0.13), flagellomeres 2–12: 0.15 (0.14–0.15), flagellomere 13: 0.06 (0.06–0.06), flagellomere 14: 0.08 (0.08–0.08); palpal segment 1: 0.04 (0.04–0.04), palpal segment 2: 0.08 (0.07–0.08), palpal segment 3: 0.07 (0.07–0.07), palpal segment 4: 0.06 (0.06–0.06).

Holotype male

Head (Fig. 8A). A little wider than long; eye bridge contiguous, with five rows of facets, interocular suture absent; post-ocular alveoli not enlarged and non-distinguishable from the remaining alveoli on the head; frontal patch of alveoli not divided, rectangular with the lower margin straight, upper margin convex. Antennal scape slightly longer than the pedicel, cylindrical; pedicel spherical; 14 flagellomeres asymmetrical and nodiform, with scattered setae on the basal half surface, apical flagellomere with terminal apiculus; ascoids about the same length as the flagellomere carrying them, and about two times wider than the width of flagellomere carrying them. Palpal segments cylindrical, palpal segment 4 apically pointed, palpal proportions: 1.0:1.8:1.6:1.4; labium without any strong sclerite; labella not bulbous with 3–4 setae on outer margin.

Thorax. Without allurement organs; all coxae with a stripe of three to five rows of alveoli. Wing length about 2.1 times its width; wing membrane brown-hyaline; alveoli distributed uniformly on wing membrane; subcostal vein short ending beyond the origin of R_4; fork of R_{2+3} basal to the level of M_{1+2} and joining R_4; fork of M_{1+2} normally sclerotized; R_5 ending at the wing apex; CuA_2 ending at wing margin.

Terminalia (Figs 8B–C, 9). Hypandrium is a distinct band that connects the gonocoxites, plate-like; gonocoxites are cylindrical, about the same length as gonostyli, gonostyli digitiform; gonocoxal apodeme fused; gonocoxal lobes without anterior projections, with 3–5 setae on each side, with gonocoxal spine; aedeagus digitiform with rounded apex, ending beyond the apex of the paramere, paramere digitiform, with rounded apex, about ¾ the length of the aedeagus; ejaculatory apodeme with anterior margin straight, shorter than the aedeagus; epandrium rectangular, about two times as wide as long; hypoproct V-shaped, and covered in small setulae, epiproct broader and shorter than hypoproct; surstyli conical narrowing towards the apex, curved ventrally, with two apical tenacula, tenacula with rounded apex.

Distribution

Only known from the type locality in Peru (Fig. 1).

DNA barcodes

No specimens were available for DNA extraction.

Bryopharsos chuspi Jaume-Schinkel sp. nov.
urn:lsid:zoobank.org:act:DCC6BE41-DA48-451D-81C3-052088A67BDD
Figs 1, 10–11

Diagnosis

Male

Eye bridge with four facet rows (Fig. 10A); wing 2.8 times as long as wide; ejaculatory apodeme about the same length as the aedeagus, with anterior margin rounded, gonocoxal apodeme projecting anteriorly;

surstyli with six apical tenacula; aedeagus digitiform, tapering towards the apex, paramere digitiform, tapering towards the apex and longer than aedeagus. This species shares the same number of apical tenacula in the surstyli as *B. gorgona* sp. nov. Still, it can be easily differentiated by the length of the hypandrium (hypandrium length is shorter than aedeagal width in *B. chuspi* sp. nov., hypandrium length is longer than aedeagal width) *B. gorgona*) and the shape of the epandrium (U-shaped in *B. chuspi*, rectangular in *B. gorgona*).

Female

Unknown.

Etymology

The specific name '*chuspi*' derives from the Quechuan word 'chuspi' meaning fly. Species name to be treated as a name in apposition.

Type material

Holotype

PERU – **Cuzco** • ♂; 26 km W of Pilcopata; alt. 1500 m; 24 Jul.–2 Aug. 1997; L.W. Quate leg.; LACM, LACM-ENT-279279.

Paratypes

PERU – **Cuzco** • 12 ♂♂; same data as for holotype; LACM, LACM-ENT-279286, LACM-ENT-279285, LACM-ENT-279284, LACM-ENT-279276, LACM-ENT-279281, LACM-ENT-279282, LACM-ENT-279283, LACM-ENT-279280, LACM-ENT-279202, LACM-ENT-279289, LACM-ENT-279288, LACM-ENT-279287.

Description

Measurements. In mm (n = 13). Wing length: 2.76 (2.50–3.00), wing width: 0.94 (0.90–1.00); head length: 0.44 (0.42–0.45), head width: 0.46 (0.46–0.48); antennal segments: scape: 0.12 (0.11–0.13), pedicel: 0.07 (0.07–0.08), flagellomere 1: 0.12 (0.11–0.12), flagellomeres 2–13: 0.14 (0.14–0.15), flagellomere 14: 0.16 (0.16–0.16); palpal segment 1: 0.06 (0.05–0.06), palpal segment 2: 0.06 (0.06–0.07), palpal segment 3: 0.08 (0.08–0.08), palpal segment 4: 0.11 (0.10–0.12).

Holotype male

Head (Fig. 10A). A little wider than long; eye bridge contiguous, with four rows of facets, interocular suture absent; post-ocular alveoli not enlarged and non-distinguishable from the remaining alveoli on the head; frontal patch of alveoli not divided, rectangular with concave lateral margins, lower margin straight, upper margin partially divided in the middle. Antennal scape is about two times as long as the pedicel, cylindrical; the pedicel is spherical; flagellomeres are asymmetrical and nodiform, with scattered setae on the basal half surface, flagellomere 14 with terminal apiculus being two times as long as the elongated basal part of the flagellomere; ascoids about the same length as the flagellomere carrying them, and about two times as wide as the width of flagellomere. Palpal segments cylindrical, palpal segment 4 apically pointed, palpal proportions: 1.0:1.0:1.3:1.8; labium without any strong sclerite; labella not bulbous with 3–4 setae on outer margin.

Thorax. Without allurement organs; all coxae with a stripe of three to five rows of alveoli. Wing length about two times its width; wing membrane brown-hyaline; alveoli distributed uniformly on wing membrane; subcostal vein short ending beyond the origin of R_4; fork of R_{2+3} basal to the level of M_{1+2} and joining R_4; fork of M_{1+2} weakly sclerotized; R_5 ending at the wing apex; CuA_2 ending at wing margin.

Terminalia (Figs 10B–C, 11). Hypandrium is a distinct band that connects the gonocoxites, plate-like; gonocoxites are cylindrical, about two-thirds the length of the gonostyli, gonostyli digitiform; gonocoxal

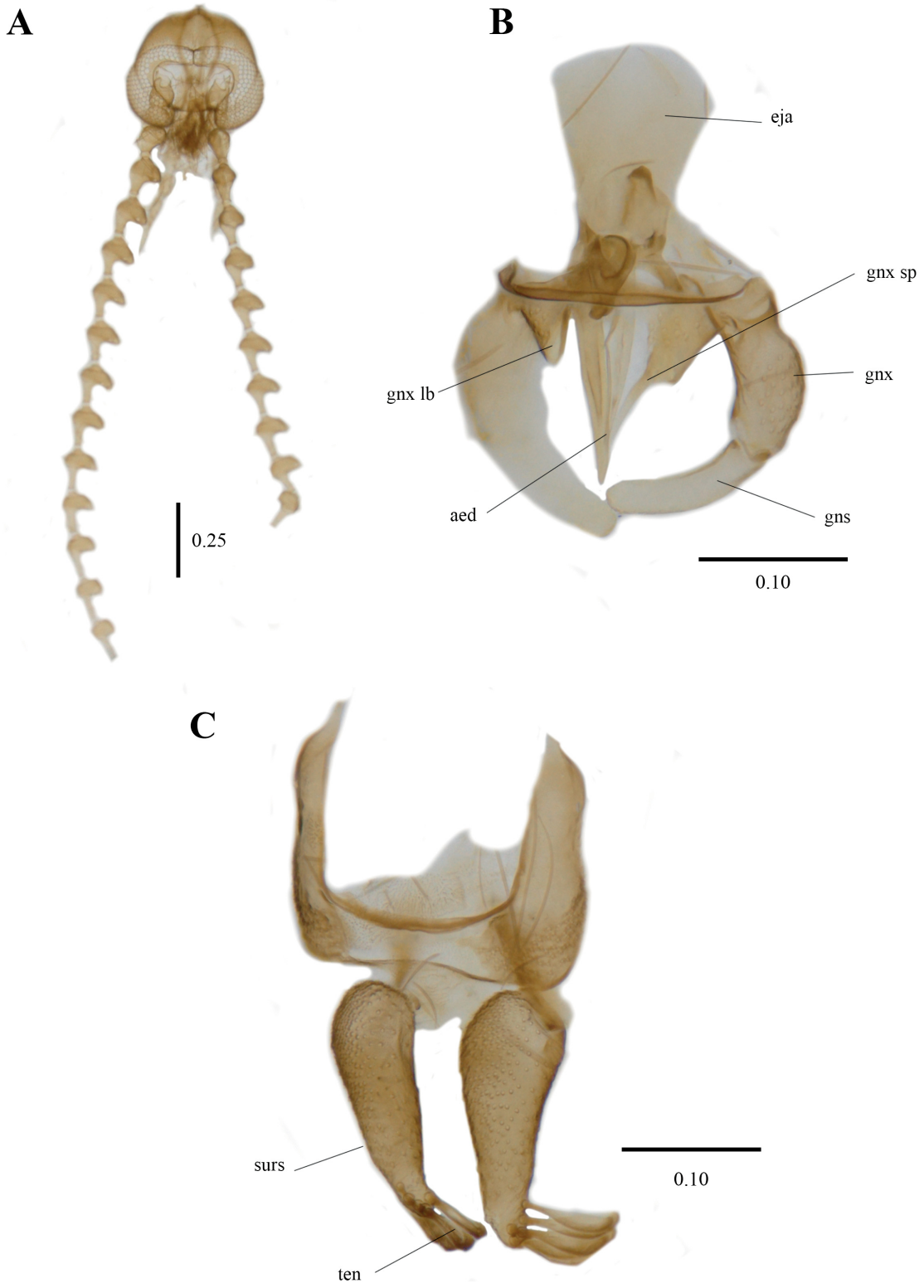

Fig. 10. *Bryopharsos chuspi* Jaume-Schinkel sp. nov., holotype, ♂ (LACM-ENT-279279). **A**. Head. **B**. Terminalia (ventral view). **C**. Surstyli. Abbreviations: aed = aedeagus; eja = ejaculatory apodeme; gns = gonostylus; gnx = gonocoxite; gnx lb = gonocoxal lobes; gnx sp = spine of the gonocoxal lobes; surs = surstylus; ten = tenacula. All scale bars are in millimeters.

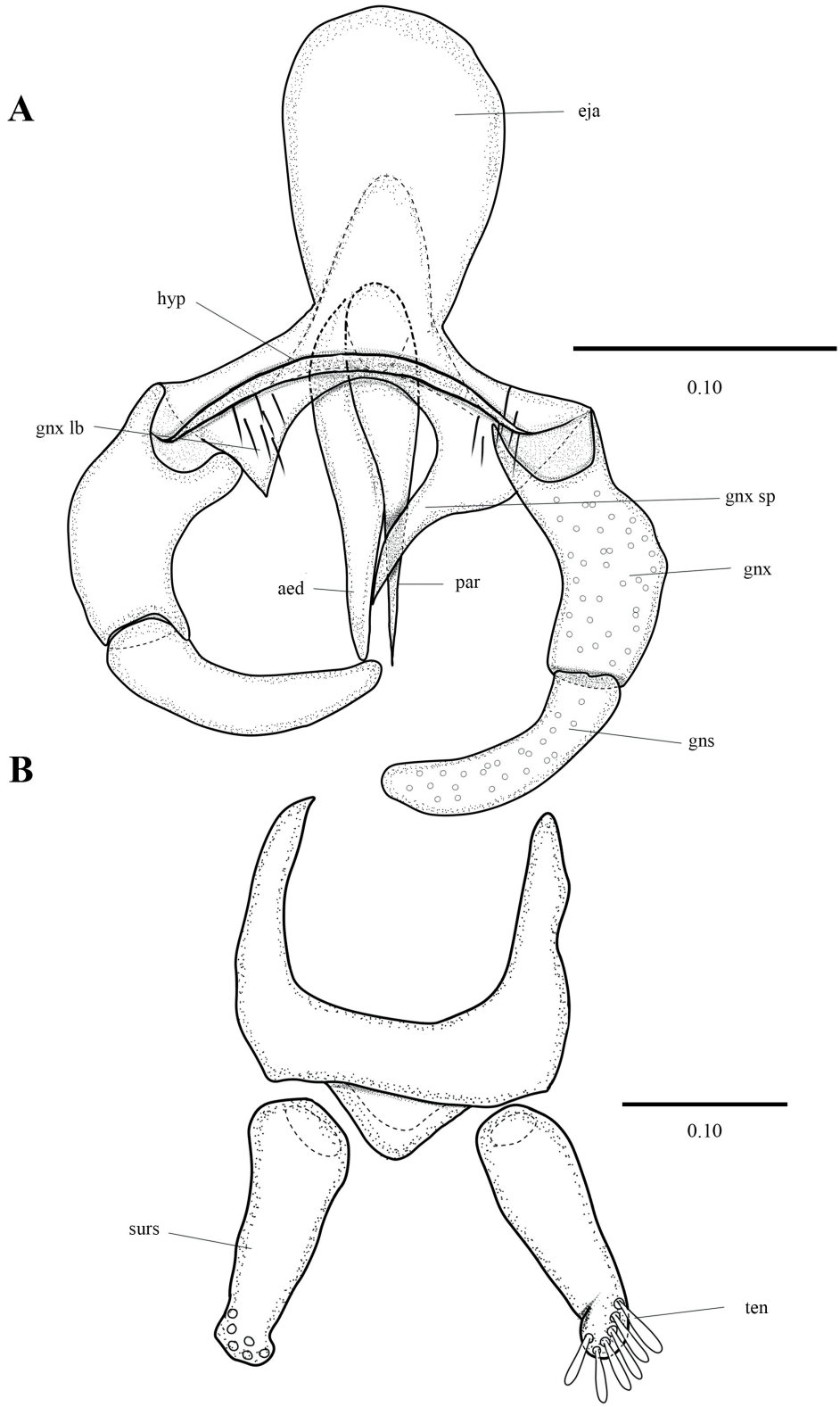

Fig. 11. *Bryopharsos chuspi* Jaume-Schinkel sp. nov., holotype, ♂ (LACM-ENT-279279). **A**. Terminalia (ventral view). **B**. Surstyli (ventral view). Abbreviations: aed = aedeagus; eja = ejaculatory apodeme; gns = gonostylus; gnx = gonocoxite; gnx lb = gonocoxal lobes; gnx sp = spine of the gonocoxal lobes; hyp = hypandrium; par = paramere; surs = surstylus; ten = tenacula. All scale bars are in millimeters.

apodeme fused; gonocoxal lobe with 5–6 setae on each side, spine of the gonocoxal lobes present; aedeagus digitiform, with rounded apex, ending at about the same level as the paramere, paramere digitiform, tapering towards apex, with pointed apex; ejaculatory apodeme with anterior margin rounded, about the same length as the aedeagus; epandrium U-shaped; hypoproct U-shaped, and covered in small setulae, epiproct broader and shorter than hypoproct; surstyli conical narrowing towards the apex, with six apical tenacula, tenacula with rounded apex.

Distribution

Only known from the type locality in Peru (Fig. 1).

DNA barcodes

No specimens were available for DNA extraction.

Bryopharsos claviformosum Quate, 1996
Figs 1, 3C–D

Bryopharsos claviformosum Quate, 1996: 41. Type locality: Costa Rica, Heredia, Estación Biológica La Selva (INBio).

Bryopharsos claviformosus – Bravo & Araújo 2019: 370 (lapsus calami in identification key).

Diagnosis

Male

Eye bridge with four facet rows; wing 2.5 times as long as wide; ejaculatory apodeme rectangular in ventral view; gonocoxal apodeme with a spine; surstyli with five tenacula. This species is similar to *B. amazonensis* and *B. clavigum* but it can be easily differentiated by the number of tenacula (four in *B. clavigum*, five in *B. amazonensis* and *B. claviformosum*) and the length of the tenacula (equal length in *B. amazonensis* and *B. clavigum*, four long and one shorter in *B. claviformosum*).

Female

Unknown.

Material examined

ECUADOR – **Pichincha** • 2 ♂♂; Pedro Vicente Maldonado, near San Pancracio, roadway to Pachijal; 0.1156° N, 78.9580° E; alt. 750 m; 1–9 Feb. 2022; Isabel Kilian leg.; ZFMK, ZFMK-TIS-2637066, ZFMK-TIS-2637079 • 1 ♂ same data as for preceding; 0.115611° N, 78.95805° E; MECN, ZFMK-TIS-2637137.

Distribution

Costa Rica (Quate 1996; Bravo & Araújo 2019) and Ecuador (this publication, new record) (Fig. 1).

DNA barcodes

Three specimens were successfully sequenced: ZFMK-TIS-2637066, ZFMK-TIS-2637079, and ZFMK-TIS-2637137. The maximum intraspecific uncorrected pairwise distance for COI sequences was 0.31% or 2 bp.

Remarks

The original description of the male by Quate (1996) is rather short and incomplete, with some important characters missing. Nonetheless, the drawings and the general description are enough to distinguish the

males of this species. In the SEM pictures (Fig. 3C–D), the aedeagus seems curved, with a rounded apex and the paramere seems digitiform and slender, while in the original description, the aedeagus looks straight and tapering towards the apex, while the paramere seems broad. We must point out that for our specimens prepared on permanent slides, the perspective affects the perceived shape of the aedeagus and paramere, making the aedeagus look straight and tapering towards the apex, and the paramere looks digitiform.

Bryopharsos clavigum Quate, 1996
Figs 1, 12

Bryopharsos clavigum Quate, 1996: 41. Type locality: Costa Rica, Heredia, Estación Biológica La Selva (INBio).

Diagnosis

Male

Eye bridge with four facet rows (Fig. 12A); wing 2.5 times as long as wide; ejaculatory apodeme sub-circular in ventral view (Fig. 12B); gonocoxal apodeme with spine (Fig. 12B); surstyli with four tenacula (Fig. 12C). This species is morphologically similar to *B. amazonensis* and *B. claviformosum* but they can be differentiated by the number of tenacula present in the surstyli (four in *B. clavigum*, five in *B. amazonensis* and *B. claviformosum*).

Female

Unknown.

Material examined

COSTA RICA – **Heredia** • 4 ♂♂; Puerto Viejo de Sarapaqui, Estación Biológica La Selva; 0.11862° N, 78.95802° E; alt. 50–100 m; 15 Dec. 1993; leg.; LACM, LACM-ENT-279401, LACM-ENT-279402, LACM-ENT-279403, INBIO CRI001470316.

ECUADOR – **Pichincha** • 1 ♂; Pedro Vicente Maldonado, near San Pancracio, roadway to Pachijal, 0.11862° N, 78.95805° E; alt. 770 m; 25–28 Jan. 2020; Isabel Kilian leg.; MECN, ZFMK-TIS-2628309.

Distribution

Costa Rica (Quate 1996; Bravo & Araújo 2019) and Ecuador (this publication, new record) (Fig. 1).

DNA barcodes

DNA barcoding of the examined material was unsuccessful.

Bryopharsos curvum Jaume-Schinkel sp. nov.
urn:lsid:zoobank.org:act:8D75061B-8145-4250-9E15-E1AA5C0BF549
Figs 1, 13

Diagnosis

Male

Eye bridge with three facet rows (Fig. 13A); wing 1.9 times as long as wide; ejaculatory apodeme cylindrical and hour-glass-shaped, about the same length as the aedeagus (Fig. 13B, D); aedeagus digitiform, outcurved and evenly tapering towards apex (Fig. 13B, D); gonocoxal apodeme fused (Fig. 13B, D); surstyli with one tenaculum (Fig. 13C). This species shares the same number of apical

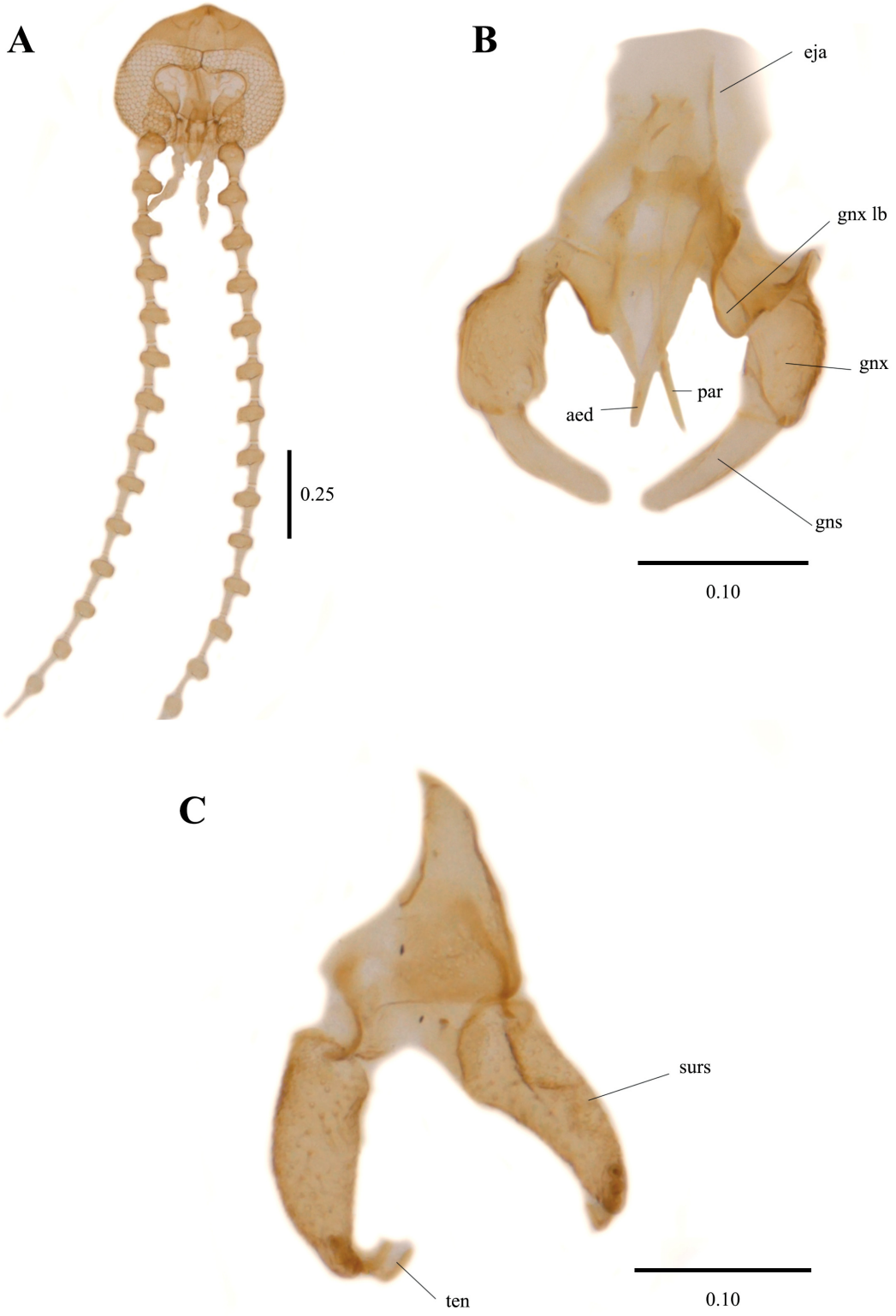

Fig. 12. *Bryopharsos clavigum* Quate, 1996, ♂ (LACM-ENT-279403). **A**. Head. **B**. Terminalia (ventral view). **C**. Surstyli (ventral view). Abbreviations: aed = aedeagus; eja = ejaculatory apodeme; gns = gonostylus; gnx = gonocoxite; gnx lb = gonocoxal lobes; par = paramere; surs = surstylus; ten = tenacula. All scale bars are in millimeters.

tenacula in the surstyli with *B. uncinatum* and *B. paulistensis*. Still, it can be easily differentiated by the number of rows of facets in the eye bridge (three in *B. curvum* sp. nov., four in *B. uncinatum*, and five in *B. paulistensis*).

Female

Unknown.

Etymology

Specific name is derived from Latin '*curvus*' (neuter 'curvum'), making reference to the outcurved gonocoxites, as well as the curved aedeagus and paramere. Specific name to be treated as a noun in apposition.

Type material

Holotype

COLOMBIA – **Magdalena** • ♂; Sierra Nevada de Santa Marta, El Ramo; alt. 2400 m; 10–24 Jun. 2000; I. Uribe leg.; Malaise trap; LACM, LACM-ENT-279396.

Description

Measurements. In mm (n = 1). Wing length: 2.47, wing width: 1.28; head length: 0.50, head width: 0.60; antennal segments: scape: 0.10, pedicel: 0.06, flagellomeres 1–4: 0.11 (0.11–0.12); palpal segment 1: 0.04, palpal segment 2: 0.8, palpal segment 3: 0.07, palpal segment 4: 0.05.

Holotype male

Head (Fig. 13A). A little wider than long; eye bridge contiguous, with three rows of facets, interocular suture absent; post-ocular alveoli not enlarged and non-distinguishable from the remaining alveoli on the head; the frontal patch of alveoli not divided, triangular with lower margin straight. Antennal scape about two times the length of the pedicel, slightly broader than wide; pedicel spherical, smaller than scape; flagellomeres asymmetrical and nodiform, with scattered setae on the basal half surface, apical flagellomeres absent in examined material, the maximum number of flagellomeres present is four; ascoids absent in examined material. Palpal segments cylindrical, palpal segment 4 with pointed apex, palpal proportions: 1.0:2.0:1.7:1.2; labium without strong sclerites; labella not bulbous with 3–4 setae on outer margin.

Thorax. Without allurement organs; all coxae with a stripe of three to five rows of alveoli. Wing length about 1.9 times its width; wing membrane brown-hyaline; alveoli distributed uniformly on wing membrane; subcostal vein short ending beyond the origin of R_4; fork of R_{2+3} at the same level as M_{1+2} and joining R_4; fork of M_{1+2} weak; R_5 ending at the wing apex; CuA_2 ending at wing margin.

Terminalia (Fig. 13B–D). Hypandrium is a distinct band that connects the gonocoxites, plate-like; gonocoxites cylindrical, shorter than gonostyli, gonostyli digitiform and outcurved, with rounded-blunt apex; aedeagus digitiform and outcurved, evenly narrowing towards the apex, apex pointed, ending at the level of the apex of the paramere, paramere digitiform and out curved, paramere evenly narrowing towards the apex, apex pointed; ejaculatory apodeme almost cylindrical, waisted and resembling a broad hour-glass shape, about the same length of the aedeagus; gonocoxal apodemes fused; epandrium like a narrow rectangle, about four times wider than long; hypoproct tongue-shaped, longer than epandrium and covered in small setulae, epiproct shorter than hypoproct; surstyli conical, evenly tapering towards the apex, with one apical tenaculum, tenaculum with rounded apex.

Distribution

Only known from the type locality in Colombia (Fig. 1).

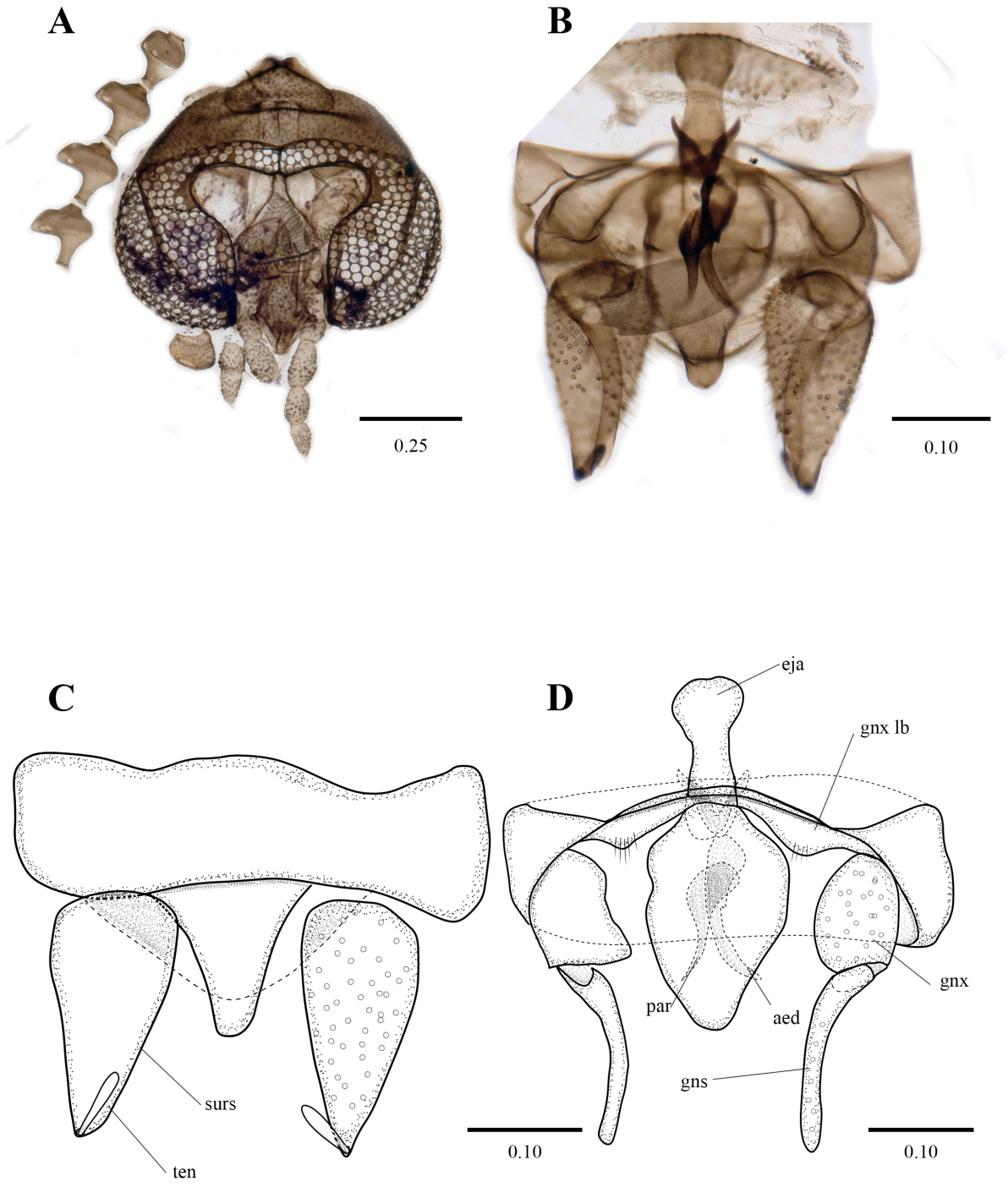

Fig. 13. *Bryopharsos curvum* Jaume-Schinkel sp. nov., holotype, ♂ (LACM-ENT-279396). **A**. Head. **B**. Terminalia (ventral view). **C**. Surstyli (ventral view). **D**. Terminalia (ventral view). Abbreviations: aed = aedeagus; eja = ejaculatory apodeme; gns = gonostylus; gnx = gonocoxite; gnx lb = gonocoxal lobes; par = paramere; surs = surstylus; ten = tenacula. All scale bars are in millimeters.

DNA barcodes

No specimens were available for DNA extraction.

Bryopharsos gorgona Jaume-Schinkel sp. nov.
urn:lsid:zoobank.org:act:7BE7FB52-C67C-417B-86AF-CCA712ADB470
Figs 1, 14

Diagnosis

Male

Eye bridge with four facet rows (Fig. 14A); wing 2.5 times as long as wide; ejaculatory apodeme short, with anterior margin straight, shorter than the aedeagus (Fig. 14B, D); gonocoxal apodeme projecting anteriorly; surstyli with six apical tenacula (Fig. 14B–C); aedeagus digitiform, with rounded apex, paramere digitiform and longer than aedeagus. This species shares the same number of apical tenacula in the surstyli as *B. gorgona* sp. nov. but it can be easily differentiated by the length of the hypandrium (hypandrium length is longer than aedeagal width in *B. gorgona*, hypandrium length is shorter than aedeagal width in *B. chuspi* sp. nov.), and the shape of the epandrium (rectangular in *B. gorgona*, U-shaped in *B. chuspi*).

Female

Unknown.

Etymology

The specific name '*gorgona*' derives from the name of the type locality, Gorgona Island. To be treated as a name in apposition.

Type material

Holotype

COLOMBIA – **Cauca** • ♂; Guapí, Gorgona Island, alta El Mirador; 2.9689° N, 78.1856° E; alt. 180 m; 4–24 Mar. 2000; R. Doque leg.; LACM, LACM-ENT-279394.

Paratypes

COLOMBIA – **Cauca** • 2 ♂♂; same data as for holotype; LACM, LACM–ENT-279395, LACM-ENT-279388.

Description

Measurements. In mm (n = 3). Wing length: 2.27 (2.204–2.55), wing width: 0.90 (0.85–0.96); head length: 0.40 (0.40–0.40), head width: 0.45 (0.45–0.45); antennal segments: scape: 0.10 (0.10–0.10), pedicel: 0.06 (0.06–0.06), flagellomere 1: 0.11 (0.11–0.12), flagellomeres 2–9: 0.12 (0.12–0.12), palpal segment 1: 0.05 (0.05–0.06), palpal segment 2: 0.07 (0.07–0.07), palpal segment 3: 0.07 (0.07–0.07), palpal segment 4: 0.08 (0.08–0.08).

Holotype male

Head (Fig. 14A). A little wider than long; eye bridge contiguous, with four rows of facets, interocular suture absent; post-ocular alveoli not enlarged and non-distinguishable from the remaining alveoli on the head; the frontal patch of alveoli not divided, rectangular with the lower and upper margins straight. Antennal scape is about two times as long as the pedicel, cylindrical; pedicel spherical; flagellomeres are asymmetrical and nodiform, with scattered setae on the basal half surface, apical flagellomeres absent, the maximum number of flagellomeres present in examined material: 9; ascoids absent in examined material.

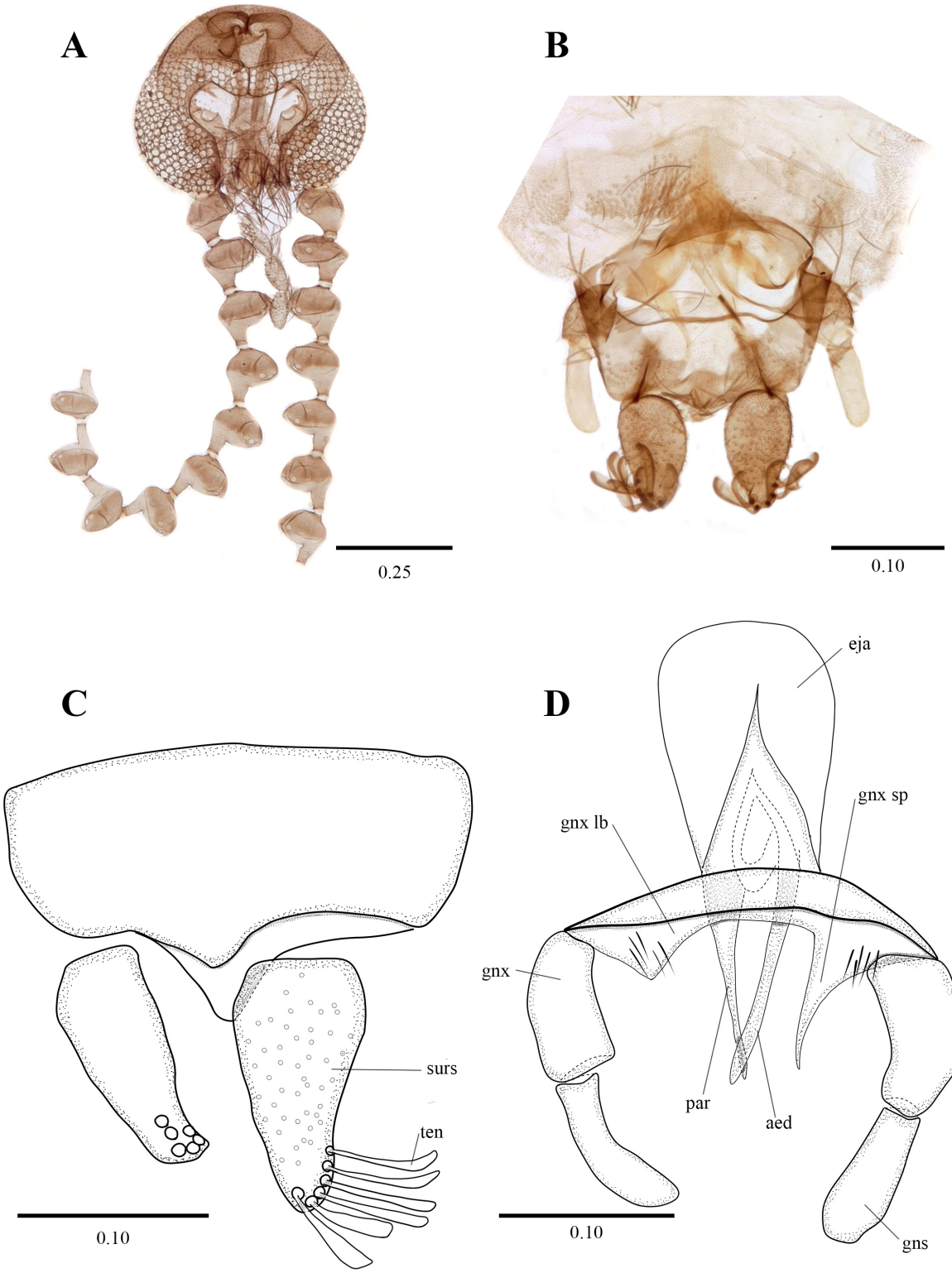

Fig. 14. *Bryopharsos gorgona* Jaume-Schinkel sp. nov., holotype, ♂ (LACM-ENT-279394). **A**. Head. **B**. Terminalia (ventral view). **C**. Surstyli (ventral view). **D**. Terminalia (ventral view). Abbreviations: aed = aedeagus; eja = ejaculatory apodeme; gns = gonostylus; gnx = gonocoxite; gnx lb = gonocoxal lobes; gnx sp = spine of the gonocoxal lobes; par = paramere; surs = surstyli; ten = tenacula. All scale bars are in millimeters.

Palpal segments cylindrical, palpal segment 4 apically pointed, palpal proportions: 1.0:1.3:1.3:1.5; labium without any strong sclerite; labella not bulbous with 3–4 setae on the outer margin.

Thorax. Without allurement organs; all coxae with a stripe of three to five rows of alveoli. Wing length about two times its width; wing membrane brown-hyaline; alveoli distributed uniformly on wing membrane; subcostal vein short ending beyond the origin of R_4; fork of R_{2+3} basal to the level of M_{1+2} and joining R_4; fork of M_{1+2} weakly sclerotized; R_5 ending at the wing apex; CuA_2 ending at wing margin.

Terminalia (Fig. 14B–D). Hypandrium is a distinct band that connects the gonocoxites, plate-like; gonocoxites are cylindrical, about two-thirds the length of the gonostyli, gonostyli digitiform; gonocoxal lobes without anterior projection, fused, and with 4–5 setae on each side; aedeagus digitiform with rounded apex, ending slightly after the apex of the paramere, paramere digitiform, evenly tapering towards apex, with pointed apex; ejaculatory apodeme with anterior margin straight, about the same length of the aedeagus; epandrium rectangular; hypoproct V-shaped, and covered in small setulae, epiproct broader and shorter than hypoproct; surstyli conical narrowing towards the apex, with six apical tenacula, tenacula with rounded apex.

Distribution

Only known from the type locality in Colombia (Fig. 1).

DNA barcodes

No specimens were available for DNA extraction.

Bryopharsos insperatum Jaume-Schinkel sp. nov.
urn:lsid:zoobank.org:act:EE933B1F-738A-48DE-9693-4129341979F4
Figs 1, 15–16

Diagnosis

Male

Eye bridge with four facet rows (Fig. 15A); wing 2.2 times as long as wide; ejaculatory apodeme cylindrical and hour-glass-shaped (Fig. 15B), about the same length as the aedeagus; gonocoxal apodeme fused; surstyli with one tenaculum (Figs 15C–D, 16B); aedeagus digitiform, out curved and evenly tapering towards apex (Fig. 16 A). This species shares the same number of apical tenaculum in the surstyli (one apical tenaculum) with *B. uncinatum* and *B. paulistensis*. Still, it can be easily differentiated by the number of rows of facets in the eye bridge (three in *B. insperatum* sp nov., four in *B. uncinatum*, and five in *B. paulistensis*).

Female

Unknown.

Etymology

The specific name '*insperatum*' derives from the Latin word '*insperatus*' (neuter '*insperatum*'), meaning unexpected, referring to unexpectedly finding a new species while looking in the collections. Name to be treated as an adjective.

Type material

Holotype

COSTA RICA – **Heredia** • ♂; Limon Rs. Biol. Hitoy Cerere, Rio Cerrere, sidestream; 9.806667° N, 83.0175° E; alt. 100–200 m; 17–26 Feb. 1999; L.W. Quate leg.; Malaise trap; LACM, INBIO CRI001473066.

Description

Measurements. In mm (n = 1). Wing length: 2.87, wing width: 1.29; head length: 0.52, head width: 0.61; antennal segments: scape: 0.14, pedicel: 0.09, flagellomere 1: 0.18, flagellomeres 2–12: 0.20; palpal segment 1: 0.07, palpal segment 2: 0.10, palpal segment 3: 0.10, palpal segment 4: 0.20.

Holotype male

Head (Fig. 15A). A little wider than long; eye bridge contiguous, with four rows of facets, interocular suture absent; post-ocular alveoli not enlarged and non-distinguishable from the remaining alveoli on the head; the frontal patch of alveoli not divided, triangular with lower margin straight. Antennal scape about two times the length of the pedicel, cylindrical; pedicel spherical, smaller than scape; flagellomeres asymmetrical and nodiform, with scattered setae on the basal half surface, apical flagellomeres absent in examined material, the maximum number of flagellomeres present is 12; ascoids rectangular and broad,

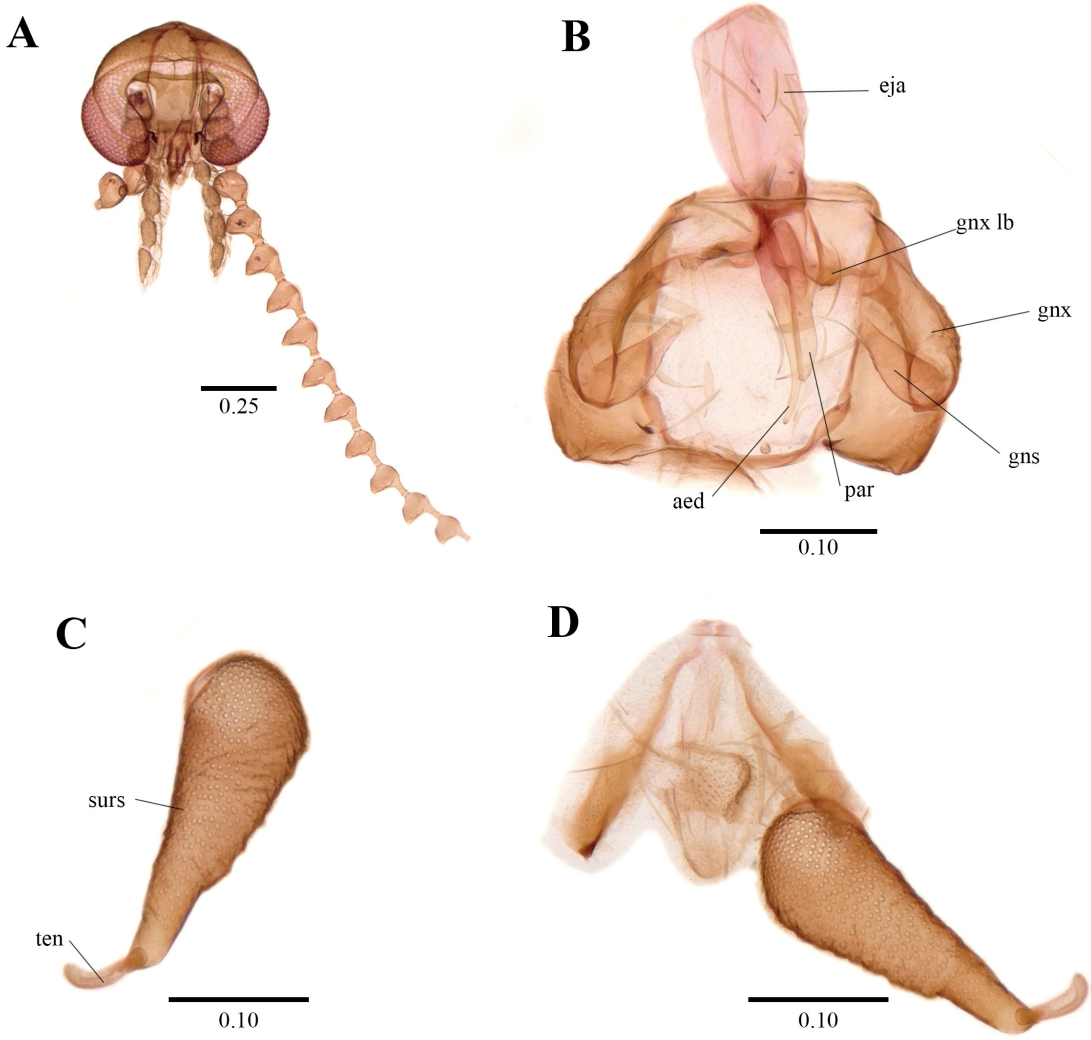

Fig. 15. *Bryopharsos insperatum* Jaume-Schinkel sp. nov., holotype, ♂ (LACM, INBIO CRI001473066). **A**. Head. **B**. Terminalia (ventral view). **C**. Surstylus. **D**. Surstylus (ventral view). Abbreviations: aed = aedeagus; eja = ejaculatory apodeme; gns = gonostylus; gnx = gonocoxite; gnx lb = gonocoxal lobes; par = paramere, surs = surstyli; ten = tenacula. All scale bars are in millimeters.

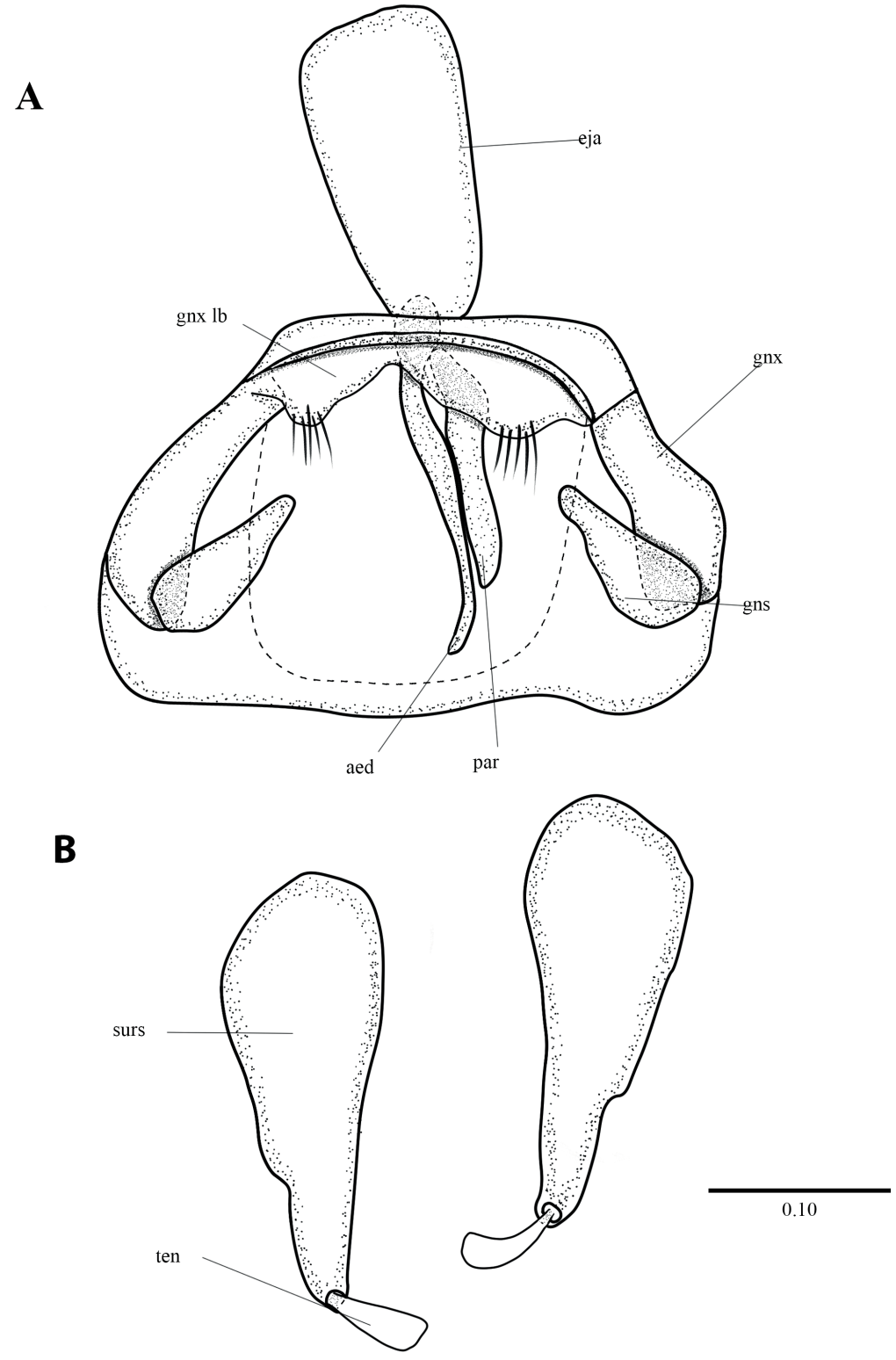

Fig. 16. *Bryopharsos insperatum* Jaume-Schinkel sp. nov., holotype, ♂ (LACM, INBIO CRI001473066). **A**. Terminalia (ventral view). **B**. Surstyli. Abbreviations: aed = aedeagus; eja = ejaculatory apodeme; gns = gonostylus; gnx = gonocoxite; gnx lb = gonocoxal lobes; par = paramere; surs = surstyli; ten = tenacula. All scale bars are in millimeters.

about the same length, and about two times as wide as flagellomere carrying them. Palpal segments cylindrical, palpal segment 4 apically pointed, with bilobed apex, palpal proportions: 1.0:1.4:1.4:2.8; labium without any strong sclerite; labella not bulbous with 3–4 setae on outer margin.

Thorax. Without allurement organs; all coxae with a stripe of three to five rows of alveoli. Wing length about 2.2 times its width; wing membrane brown-hyaline; alveoli distributed uniformly on wing membrane; subcostal vein short ending beyond the origin of R_4; fork of R_{2+3} at the basal to the level of M_{1+2} and joining R_4; fork of M_{1+2} weakly sclerotized, almost appears as it is not joining; R_5 ending at the wing apex; CuA_2 ending at wing margin.

Terminalia (Figs 15B–D, 16). Hypandrium is a distinct band that connects the gonocoxites, plate-like; gonocoxites cylindrical, longer than gonostyli, gonostyli conical, with rounded-blunt apex; gonocoxal apodeme not anteriorly projected; gonocoxal lobes posteriorly projected on each side, each lobe with five setae; aedeagus digitiform and out curved, evenly narrowing towards the apex, apex rounded, and ending beyond the apex of the paramere, paramere digitiform (Fig. 16A), broader than aedeagus, with apex rounded; ejaculatory apodeme with anterior margin round (Fig. 16A), about the same length of the aedeagus; epandrium not discernable in examined material, but appears U-shaped; hypoproct tongue-shaped (Fig. 15D), and covered in small setulae, epiproct shorter than hypoproct; surstyli conical, slightly tapering towards the apex and curved ventrally, with one apical tenaculum, tenaculum with rounded apex.

Distribution

Only known from the type locality in Costa Rica (Fig. 1).

DNA barcodes

No specimens were available for DNA extraction.

Bryopharsos palpiculum Quate, 1996
Figs 1, 17–18

Bryopharsos palpiculum Quate, 1996: 41. Type locality: Costa Rica, Heredia, Estación Biológica La Selva (INBio).

Diagnosis

Male

Eye bridge with five facet rows (Fig. 17A); wing 2.4 times as long as wide; ejaculatory apodeme sub-circular in ventral view; gonocoxal apodeme with a spine-shaped projection; surstyli with four tenacula (Fig. 17C); aedeagus long and straight, narrowing at the apex (Fig. 17B). This species shares five face rows with *B. paulistensis* but they can be easily differentiated by the number of tenacula on the surstyli (four in *B. palpiculum*, one in *B. paulistensis*).

Female (adapted from Quate 1999)

Subgenital plate with slender constriction before small apical lobes, triangular in shape before constriction; membranous plate indistinct; genital chamber faint, without distinct structure, appears as a spherical structure partially divided apically (see Quate 1999: 434–435, fig. 7c).

Material examined

COSTA RICA – **Heredia** • 6 ♂♂; Puerto Viejo de Sarapaqui, Estación Biológica La Selva; 0.11862° N, 78.95802° E; alt. 50–100 m; 15 Dec. 1993; LACM, INBIO CRI001470484, INBIO CRI001470634, INBIO CRI001470595, INBIO CRI001470134, INBIO CRI001470343, INBIO CRI001470240.

ECUADOR – **Pichincha** • 1 ♂; Pedro Vicente Maldonado, near San Pancracio, roadway to Pachijal; 0.11862° N, 78.95805° E; alt. 770 m; 25–28 Jan. 2020; Isabel Kilian leg.; MECN, ZFMK-TIS-2628311 • 1 ♀; same data as for preceding; ZFMK, ZFMK-TIS-2629904 • 2 ♂♂; same data as for preceding; 0.1156° N, 78.9580° E; alt. 750 m; 1–9 Feb. 2022; ZFMK, ZFMK-TIS-2637073, ZFMK-TIS-2637080 • 1 ♂; MECN, ZFMK-TIS-2637071.

NICARAGUA – **Rio San Juan** • 5 ♂♂ SE of San Carlos; 10.9666° N, 84.3333° E; alt. 30 m; 6–10 Feb. 2000; L.W. Quate leg.; Malaise trap; lowland rain forest; LACM LACM-ENT-279365, LACM-ENT-279366, LACM-ENT-279367, LACM-ENT-279368, LACM-ENT-279369.

PANAMA – **Canal Zone** • 1 ♂; Barro Colorado Island; 9.1500° N, 79.8500° E; 11–18 Aug. 1993; J. Pickering leg.; LACM, LACM-ENT-279380 • 1 ♂; same collection data as for preceding; 28 Jul.–4 Aug. 1993; LACM • 1 ♂; same data as for preceding; 31 Jan.–7 Feb. 1996; LACM, LACM-ENT-279374 • 1 ♂; same data as for preceding; 6–13 Oct. 1996; LACM, LACM-ENT-279373 • 1 ♂; same data as for

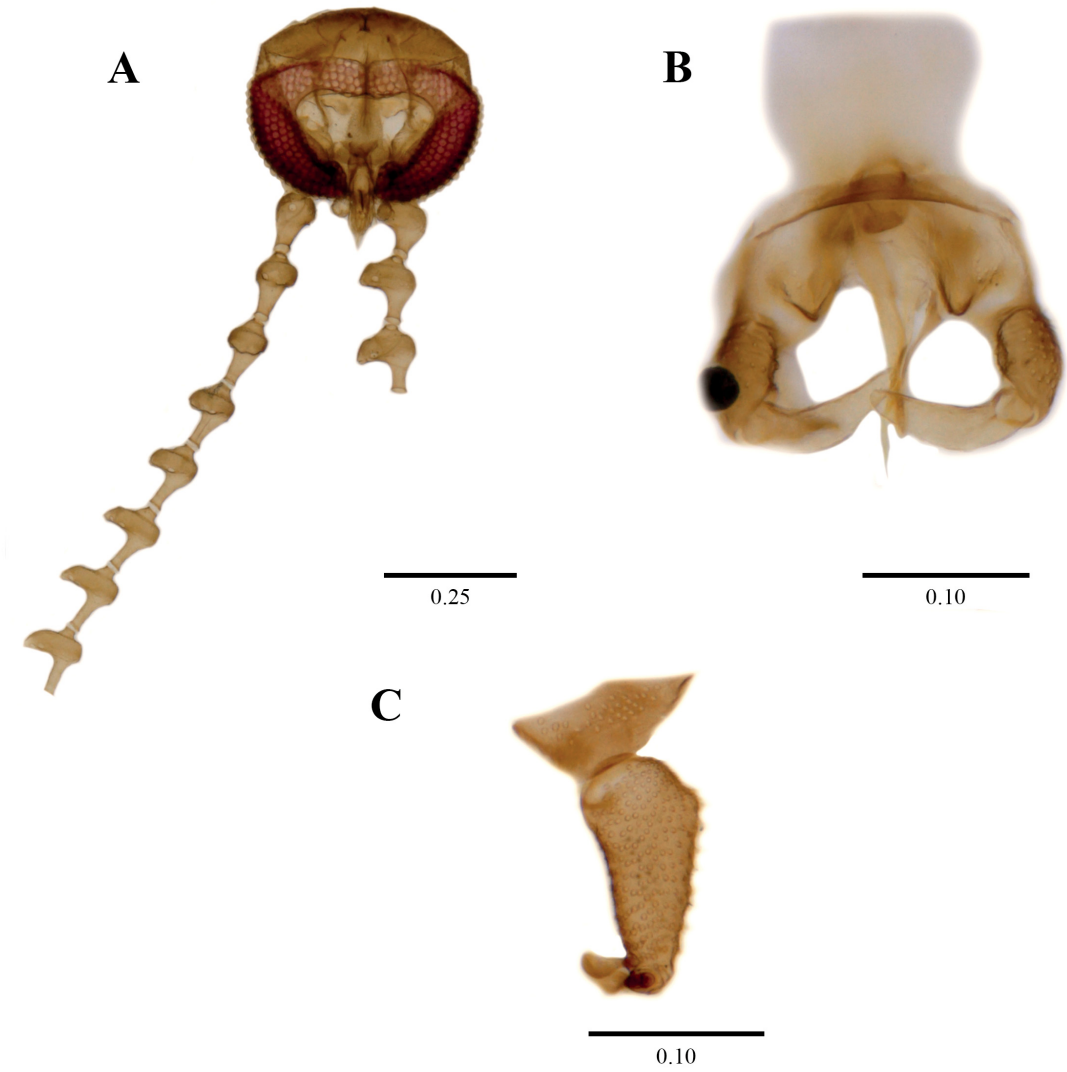

Fig. 17. *Bryopharsos palpiculum* Quate, 1996, ♂ (LACM, INBIO CRI001470240). **A**. Head. **B**. Terminalia (ventral view). **C**. Surstyli. All scale bars are in millimeters.

preceding; 23–30 Oct. 1996; LACM, LACM-ENT-279372 • 1 ♂; same data as for preceding; 18–27 Dec. 1996; LACM, LACM-ENT-279370 • 1 ♂; same data as for preceding; 1996; LACM, LACM-ENT-279378. – **Guna Yala** (previously known as San Blas) • 1 ♂; Nusagandi Reserve; 9.3333° N, 79.0000° E; 12–19 Feb. 1994; J. Pickering leg; LACM, LACM-ENT-279377 • 3 ♂♂; same data as for preceding; 24 Jun.–4 Jul. 1993; LACM, LACM-ENT-279371; LACM-ENT-279379; LACM-ENT-279376.

Redescription

Female

Head. About as long as wide, eye bridge contiguous with four facet rows; interocular suture absent; five enlarged post-ocular alveoli on each lateral margin; frontal patch of alveoli undivided, triangular with rounded vertices. Antennal scape about 1.5 times as long as the pedicel, cylindrical; pedicel spherical, shorter than scape; flagellomeres smaller than male flagellomeres, asymmetrical-podiform, apical flagellomeres missing in examined material; palpal segments cylindrical, apical palpal segment with pointed apex; palpal proportions: 1.0:1.2:1.2:1.5.

Thorax. Without allurement organs. Wing. 2.3 times as long as wide, wing membrane brown-hyaline, alveoli distributed uniformly on wing membrane; subcostal vein short ending beyond the origin of R_4; fork of R_{2+3} at the same level as M_{1+2} and joining R_4; fork of M_{1+2} weak; R_5 ending at the wing apex; CuA_2 ending at wing margin. Tergite nine with apical lobes (Fig. 18A), broad and digitiform, about the same length as tergite nine; subgenital plate membranous except for apical lobes which are sclerotized, basal margin round, with a constriction before apical lobes; genital chamber membranous, barely visible; cerci short, about the same length as the subgenital plate.

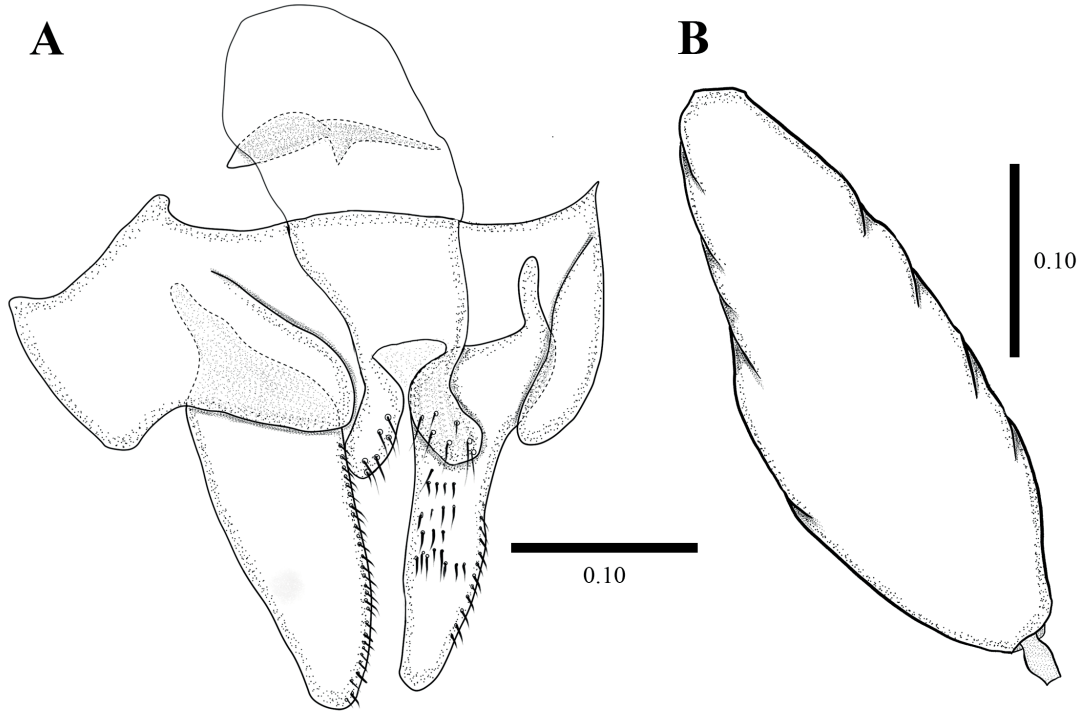

Fig. 18. *Bryopharsos palpiculum* Quate, 1996, (ZFMK-TIS-2629904). ♀ **A**. Terminalia (ventral view). **B**. Egg. All scale bars are in millimeters.

Egg (Fig. 18B). Length 0.336 ± 0.020 mm. Width 0.14 ± 0.032 mm (n = 8). No exochorion sculptures where observed along the long axis of the egg. No aeropiles were observed in the posterior pole. The anterior pole presents a cylindrical projection of about 0.02 mm, with a truncated apex, without exochorion sculptures.

Distribution

Costa Rica, Panama (Quate 1996; Bravo & Araújo 2019), and Ecuador (this publication, new record) (Fig. 1).

DNA barcodes

Five specimens were successfully sequenced: ZFMK-TIS-2628311, ZFMK-TIS-2629904, ZFMK-TIS-2637071, ZFMK-TIS-2637073, ZFMK-TIS-2637080. The maximum intraspecific uncorrected pairwise distance for COI sequences was 1.07% or 7 bp.

Remarks

Quate (1996) originally described *B. palpiculum* based on male specimens. Later, he (Quate 1999) described the females collected in Nusagandi Reserve (Panama) appealing to the co-occurrence of these female specimens with males of *B. palpiculum*. These females were the first known and reported female specimens of *Bryopharsos*. The female description is relatively brief and the illustration only shows the genital chamber and the subgenital plate.

In this study, the association between the examined male and female specimens was done using the DNA barcodes (see section above). Our specimen differs from that on the drawings provided by Quate (1999), i.e., in specimen ZFMK-TIS-2637073 the paramere looks shorter than in Quate's drawing while in specimen ZFMK-TIS-2637080, the paramere is strongly curved (although the shape/position likely changed during the mounting process). In specimen ZFMK-TIS-2637071, the base of the paramere looks broader than on Quate's drawing, but the general morphology is similar. The variation can be explained by the angle in which the terminalia were prepared on the microscope slides, but when comparing with other specimens deposited in other collections there is no doubt they all belong to the same species.

Bryopharsos paulistensis Bravo & Araújo, 2019
Figs 1, 19

Bryopharsos paulistensis Bravo & Araújo, 2019: 365. Type locality: Brazil, São Paulo, Sete Barras (MZFS).

Diagnosis

Male

Eye bridge of five facet rows (Fig. 19A); wing two times as long as wide; ejaculatory apodeme sub-rectangular in ventral view (Fig. 19B); gonocoxal apodeme with anterior projection as a lobe (Fig. 19B); surstyli with one tenaculum (Fig. 19C); aedeagus long and expanded, hemispheric basally and narrowly pointed at the apex (Fig. 19B). This species is similar to *B. uncinatum*, both can be easily differentiated by the number of facet rows in the eye bridge (four in *B. uncinatum*, five in *B. paulistensis*).

Female

Unknown.

Material examined

None.

Distribution

Brazil (Bravo & Araújo 2019) (Fig. 1).

DNA barcodes

No specimens were available for DNA extraction.

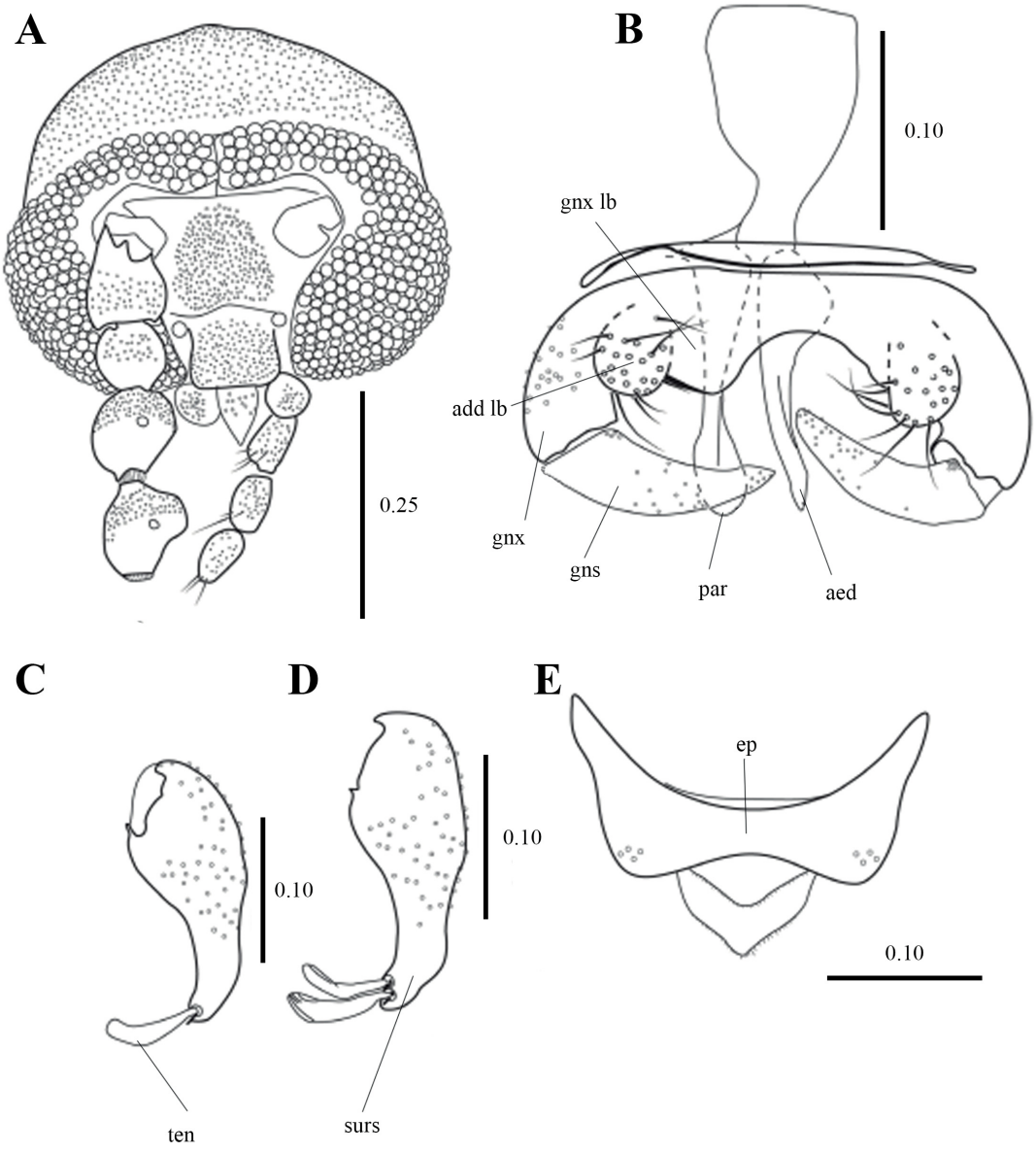

Fig. 19. *Bryopharsos paulistensis* Bravo & Araujo, 2019, ♂. **A**. Head. **B**. Terminalia (ventral view). **C–D**. Surstyli. **E**. Epandrium. Abbreviations: add lb = additional lobe of gonocoxal lobe; aed = aedeagus; ep = epandrium; gns = gonostylus; gnx = gonocoxite; gnx lb = gonocoxal lobes; par = paramere; surs = surstyli; ten = tenacula. All scale bars are in millimeters. Figures adapted from Bravo & Araujo (2019) with permission of the copyright holder © Magnolia Press.

Bryopharsos septenacula Jaume-Schinkel sp. nov.
urn:lsid:zoobank.org:act:D9D297C4-05C9-4217-9EB0-9E0355EB9FB2
Figs 1, 20–21

Diagnosis

Male

Eye bridge with four facet rows (Fig. 20A); wing 2.1 times as long as wide; ejaculatory apodeme oval, about the same length as the aedeagus (Figs 20B, 21); gonocoxal apodeme with spine-like anterior projection; surstyli with seven tenacula (Figs 20B, 21); aedeagus digitiform and evenly tapering towards apex, and ending before the apex of paramere (Fig. 21), paramere shaped as an inverted J (Fig. 21B). This species shares the same number of facet rows in the eye bridge as *B. uncinatum*, *B. tritaleum*, *B. clavigum*, *B. amazonensis*, and *B. claviformosum*, but it can be easily differentiated by the number of tenacula on the surstyli (seven in *B. septenacula* sp. nov., five in *B. amazonensis* and *B. claviformosum*, one in *B. uncinatum*, and four in *B. tritaleum*).

Female

Unknown.

Etymology

The specific name derives from the Latin words '*septem*' meaning seven, and '*tenaculum*' (plural '*tenacula*'), the so-called stiff flattened setae on the inner apical surface of the surstyli of many Psychodidae. The name makes reference to the number of tenacula present in the species. Specific name to be treated as name in apposition.

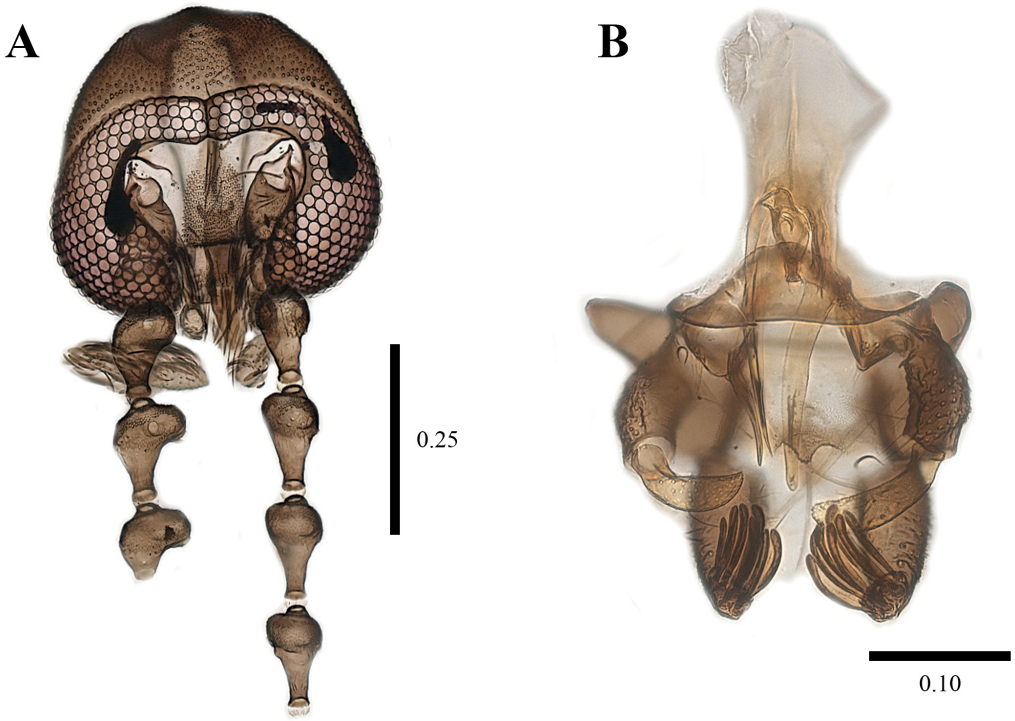

Fig. 20. *Bryopharsos septenacula* Jaume-Schinkel sp. nov., holotype, ♂ (MECN, ZFMK-TIS-2637106). **A**. Head. **B**. Terminalia (ventral view). All scale bars are in millimeters.

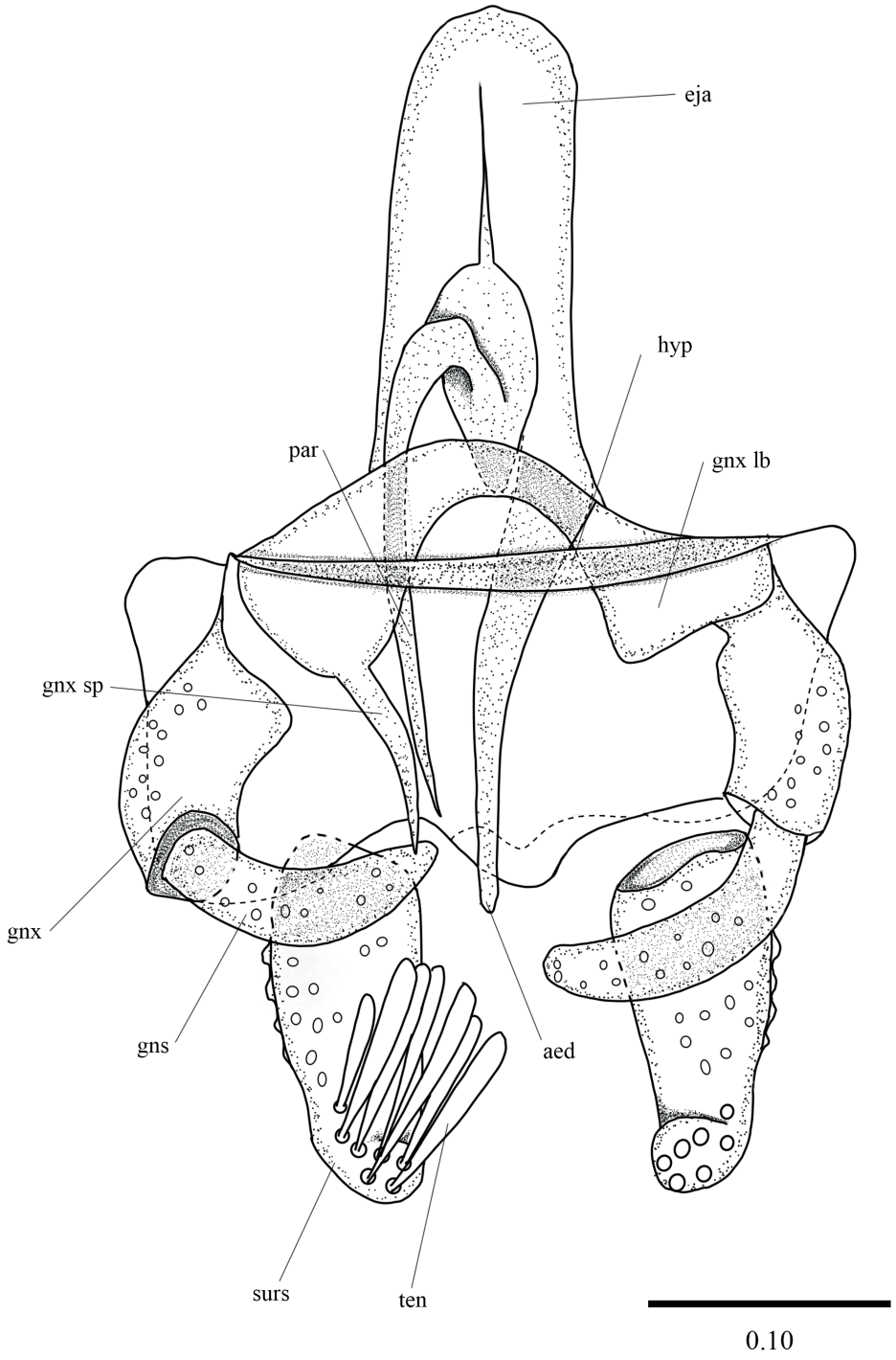

Fig. 21. *Bryopharsos septenacula* Jaume-Schinkel sp. nov., holotype, ♂ (MECN, ZFMK-TIS-2637106). Terminalia (ventral view). Abbreviations: aed = aedeagus; eja = ejaculatory apodeme; gns = gonostylus; gnx = gonocoxite; gnx lb = gonocoxal lobes; gnx sp = spine of gonocoxal lobe; hyp = hypandrium; par = paramere; surs = surstyli; ten = tenacula. Scale bar in millimeters.

Type material

Holotype

ECUADOR – **Pichincha** • ♂; Pedro Vicente Maldonado, Parroquia Pedro Vicente Maldonado, near San Pancracio, roadway to Pachijal; 0.11561° N, 78.95805° E; alt. 750 m; 1–9 Feb. 2022; Isabel Kilian leg.; MECN, ZFMK-TIS-2637106.

Paratypes

ECUADOR – **Pichincha** • 5 ♂♂; same data as for holotype; ZFMK, ZFMK-TIS-2637088, ZFMK-TIS-2637153, ZFMK-TIS-2637157, ZFMK-TIS-2637174, ZFMK-TIS-2637170 • 1 ♂; same data as for holotype; MECN, ZFMK-TIS-2637178 • 1 ♂; same data as for holotype; 0.11862° N, 78.95805° E; alt. 770 m; 30 Dec. 2021–5 Jan. 2022; ZFMK, ZFMK-TIS-2636933. – **Esmeraldas** • 1 ♂; Parroquia San Francisco del Cabo, canton Bunche; 0.64562° N, 80.0253° E; alt. 46 m; 30 Dec. 2021–5 Jan. 2022; ZFMK, ZFMK-TIS-2636988 • 2 ♂♂; same data as for preceding; 25–28 Jan. 2020; ZFMK, ZFMK-TIS-2629871, ZFMK-TIS-2629873.

Description

Measurements. In mm (n = 5). Wing length: 1.70 (1.80–1.50), wing width: 0.79 (0.80–0.72); head length: 0.40 (0.40), head width: 0.35 (0.35); antennal segments: scape: 0.10 (0.11–0.08), pedicel: 0.06 (0.06–0.05), flagellomeres 1–7: 0.1 (0.11–0.10); palpal segment 1: 0.05 (0.5), palpal segment 2: 0.07 (0.07), palpal segment 3: 0.07 (0.07), palpal segment 4: 0.07 (0.07).

Holotype male

Head (Fig. 20A). A little wider than long; eye bridge contiguous, with four rows of facets, interocular suture absent; post-ocular alveoli not enlarged and non-distinguishable from the remaining alveoli on the head; the frontal patch of alveoli not divided, trapezoidal with upper and lower margins straight. Antennal scape about two times the length of the pedicel, almost cylindrical; pedicel spherical, smaller than scape; flagellomeres asymmetrical and nodiform, with scattered setae on the basal half surface, apical flagellomeres absent in examined material, the maximum number of flagellomeres present seven; ascoids rectangular and broad, about the same length, and about two times as wide as flagellomere carrying them. Palpal segments cylindrical, palpal segment 4 with pointed apex, palpal proportions: 1.0:1.5:1.5:1.5; labium without any strong sclerite; labella not bulbous with 3–4 setae on outer margin.

Thorax. Without allurement organs; all coxae with a stripe of three to five rows of alveoli. Wing length about 2.1 times its width; wing membrane brown-hyaline; alveoli distributed uniformly on wing membrane; subcostal vein short ending beyond the origin of R_4; fork of R_{2+3} at the same level as M_{1+2} and joining R_4; fork of M_{1+2} weak; R_5 ending at the wing apex; CuA_2 ending at wing margin.

Terminalia (Figs 20B, 21). Hypandrium is a distinct band that connects the gonocoxites, plate-like; gonocoxites about the same length as gonostyli, gonostyli slightly incurved, with rounded-blunt apex; aedeagus digitiform, evenly narrowing towards the apex, apex rounded, ending beyond the level of the paramere, paramere resembling an inverted 'J' (Fig. 21), apex pointed; ejaculatory apodeme oval, about the same length as the aedeagus, anterior margin rounded; gonocoxal apodemes projected anteriorly and fused, resembling an inverted and wide 'U', spine of the gonocoxal lobes present; epandrium narrow, rectangular, about three times as wide long; hypoproct digitiform, shorter than epandrium and covered in small setulae, epiproct shorter than hypoproct; surstyli conical, slightly tapering towards the apex and curved ventrally, with seven apical tenacula, tenacula with rounded apex.

Distribution

Only known from the type locality in Ecuador (Fig. 1).

DNA barcodes

Eleven specimens were successfully sequenced ZFMK-TIS-2629871, ZFMK-TIS-2629873, ZFMK-TIS-2636933, ZFMK-TIS-2636988, ZFMK-TIS-2637088, ZFMK-TIS-2637106, ZFMK-TIS-2637153, ZFMK-TIS-2637157, ZFMK-TIS-2637170, ZFMK-TIS-2637174, and ZFMK-TIS-2637178. The maximum intraspecific uncorrected pairwise distance for COI sequences was 0.46% or 2 bp.

Bryopharsos tetracanthus Jaume-Schinkel sp. nov.
urn:lsid:zoobank.org:act:635E31CD-1373-4E14-B29E-381911CCAE3C
Figs 1, 22

Diagnosis

Male

Eye bridge with four facet rows (Fig. 22A); wing 2.4 times as long as wide; ejaculatory apodeme cylindrical and hour-glass-shaped (Fig. 22B), about the same length as the aedeagus (Fig. 22D); gonocoxal apodeme fused; surstyli with three apical tenacula (Fig. 22B–C); aedeagus digitiform, curved and evenly tapering towards apex (Fig. 22D). This species shares the same number of apical tenacula in the surstyli (three tenacula) with *B. tritaleum* but it can be easily differentiated by the distribution of the apical tenacula in the surstyli (closely together at the apex in *B. tetracanthus* sp. nov., 2 apical tenacula separated from 1 basal tenaculum in *B. tritaleum*), and the shape of the aedeagus (digitiform and curved in *B. tetracanthus*, digitiform and straight in *B. tritaleum*).

Female

Unknown.

Etymology

The specific name '*tetracanthus*' derives from the Greek word 'τετρα-' ('tetra-') as a prefix, meaning four, and the Greek word 'ἄκανθος' ('ákanthos'), meaning spine. The specific name makes reference to the four spines located in between the apical tenacula in the surstyli. Specific name to be treated as a name in apposition.

Type material

Holotype

COLOMBIA – **Magdalena** • ♂; Sierra Nevada de Santa Maria, El Ramo; alt. 2400 m; 10–24 May 2000; I. Uribe leg.; Malaise trap; LACM, LACM-ENT-279397.

Description

Measurements. In mm (n = 1). Wing length: 1.92, wing width: 0.80; head length: 0.39, head width: 0.46; antennal segments: scape: 0.08, pedicel: 0.06, flagellomeres 1–4: 0.11; palpal segment 1: 0.05, palpal segment 2: 0.06, palpal segment 3: 0.06, palpal segment 4: 0.07.

Holotype male

Head (Fig. 22A). A little wider than long; eye bridge contiguous, with four rows of facets, interocular suture absent; post-ocular alveoli not enlarged and non-distinguishable from the remaining alveoli on the head; the frontal patch of alveoli not divided, trapezoidal with the lower margin with a concavity in the middle. Antennal scape about the same length as pedicel, cylindrical; pedicel spherical, about the same length as scape; flagellomeres asymmetrical and nodiform, with scattered setae on the basal half surface, apical flagellomeres absent in examined material, the maximum number of flagellomeres present is seven; ascoids absent in examined material. Palpal segments cylindrical, palpal segment 4 apically pointed, palpal proportions: 1.0:1.2:1.2:1.4; labium without any strong sclerite; labella not bulbous with 3–4 setae on outer margin.

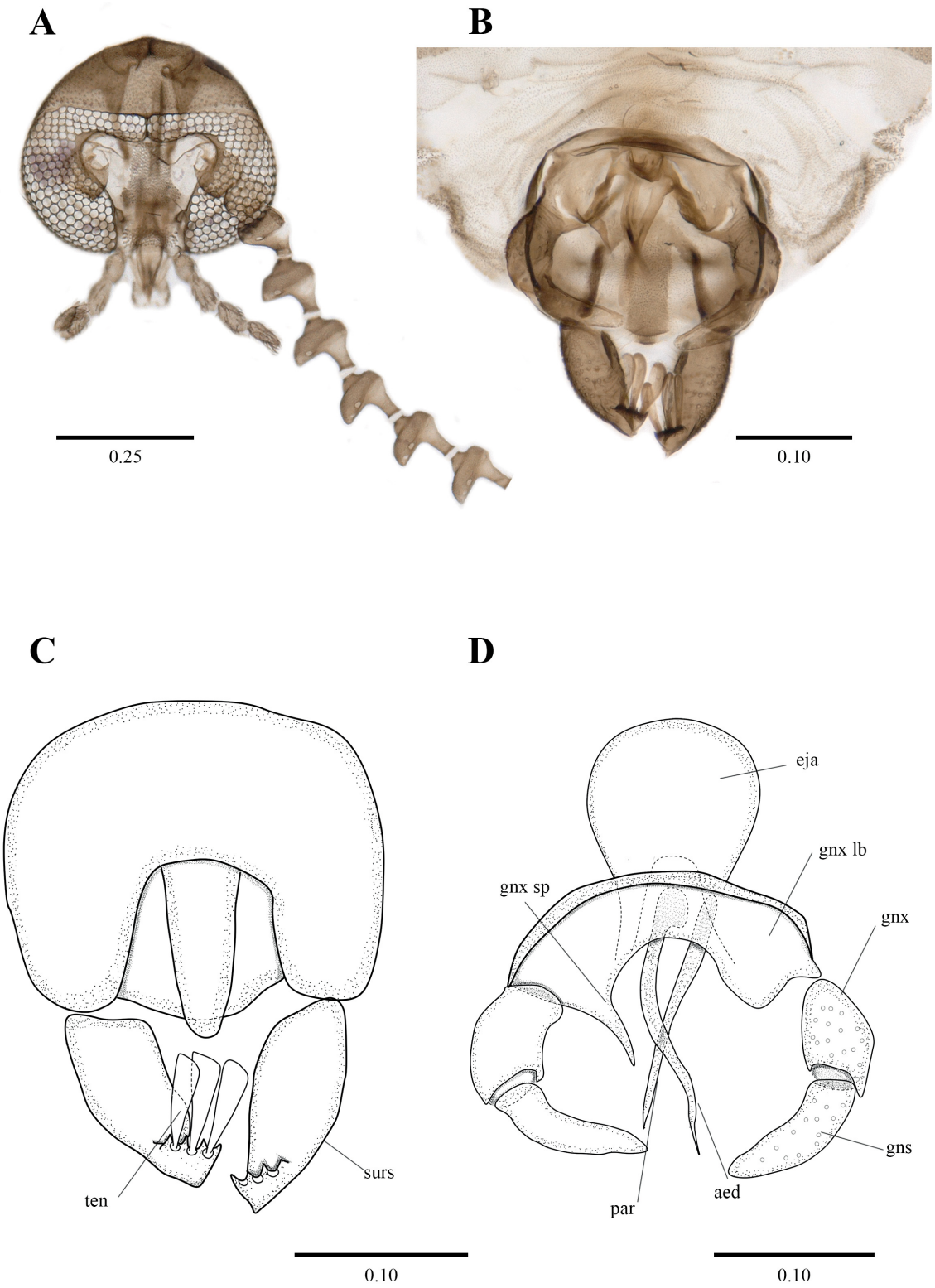

Fig. 22. *Bryopharsos tetracanthus* Jaume-Schinkel sp. nov., holotype, ♂ (LACM-ENT-279397). **A**. Head. **B**. Terminalia (ventral view). **C**. Epandrium and surstyli. **D**. Terminalia (ventral view). Abbreviations: aed = aedeagus; eja = ejaculatory apodeme; gns = gonostylus; gnx = gonocoxite; gnx lb = gonocoxal lobes; gnx sp = spine of gonocoxal lobe; par = paramere; surs = surstyli; ten = tenacula. All scale bars are in millimeters.

Thorax. Without allurement organs; all coxae with a stripe of three to five rows of alveoli. Wing length about 2.4 times its width; wing membrane brown-hyaline; alveoli distributed uniformly on wing membrane; subcostal vein short ending beyond the origin of R_4; fork of R_{2+3} at the same level as M_{1+2} and joining R_4; fork of M_{1+2} normally sclerotized; R_5 ending at the wing apex; CuA_2 ending at wing margin.

Terminalia (Fig. 22B–D). Hypandrium is a distinct band that connects the gonocoxites, stripe-like; gonocoxites cylindrical, shorter than gonostyli, gonostyli digitiform, with rounded apex; gonocoxal apodeme anteriorly projected with rectangular anterior margin; gonocoxal lobes with four setae on each side, spine of the gonocoxal lobes present; aedeagus digitiform and curved, evenly narrowing towards the apex, apex pointed, ending beyond the apex of the paramere, paramere digitiform, rounded at apex; ejaculatory apodeme with anterior margin rounded, shorter than the length of the aedeagus; epandrium plate-like, square and resembling an inverted U (Fig. 22C); hypoproct elongated, almost thumb-like, about three times as long as wide, and covered in small setulae, epiproct shorter than hypoproct, about as wide as long; surstyli conical, tapering towards the apex and curved ventrally, with three close-together apical tenacula, tenacula with rounded apex, with additional 4 spiniform projections in-between the tenacula (Fig. 22B–D).

Distribution

Only known from the type locality in Colombia (Fig. 1).

DNA barcodes

No specimens were available for DNA extraction.

Bryopharsos tritaleum Quate, 1996
Figs 1, 23

Bryopharsos tritaleum Quate, 1996: 41. Type locality: Costa Rica, Heredia, Estación Biológica La Selva (INBio).

Diagnosis

Male

Eye bridge with four facet rows; wing 2.2 times as long as wide; ejaculatory apodeme ovoid in ventral view; gonocoxal apodeme with a spine-shaped projection (Fig. 23A); surstyli with three tenacula (Fig. 23B); aedeagus straight with a pointed apex (Fig. 23A). This species is similar to *B. asymmetricum* sp. nov. They can be easily differentiated by the number of facet rows in the eye bridge (four in *B. tritaleum*; five in *B. asymmetricum*), and the length of the ejaculatory apodeme (about as long as the aedeagus in *B. tritaleum*; shorter than the aedeagus in *B. asymmetricum*).

Female

Unknown.

Material examined

None.

Distribution

Costa Rica (Quate 1996; Bravo & Araújo 2019) (Fig. 1).

DNA barcodes

No specimens were available for DNA extraction.

Bryopharsos uncinatum Bravo & Araújo, 2019
Figs 1, 24

Bryopharsos uncinatum Bravo & Araújo, 2019: 365. Type locality: Brazil, São Paulo, Sete Barras (MZFS).

Diagnosis

Male

Eye bridge with four facet rows (Fig. 24A); wing two times as long as wide; ejaculatory apodeme subcircular in ventral view; gonocoxal apodeme without anterior projection (Fig. 24B); surstyli with one tenaculum (Fig. 24C); aedeagus hook-shaped (Fig. 24B). This species is similar to *B. paulistensis* with both species presenting only one tenaculum in the surstyli (the other species present 3–7 tenacula), but they can be differentiated by the number of facet rows in the eye bridge (four in *B. uncinatum*, five in *B. paulistensis*) and the spine of the gonocoxal apodeme (absent in *B. uncinatum*, present in *B. paulistensis* as rounded projections (referred to as lobes in Bravo & Araújo 2019)).

Female

Unknown.

Material examined

None.

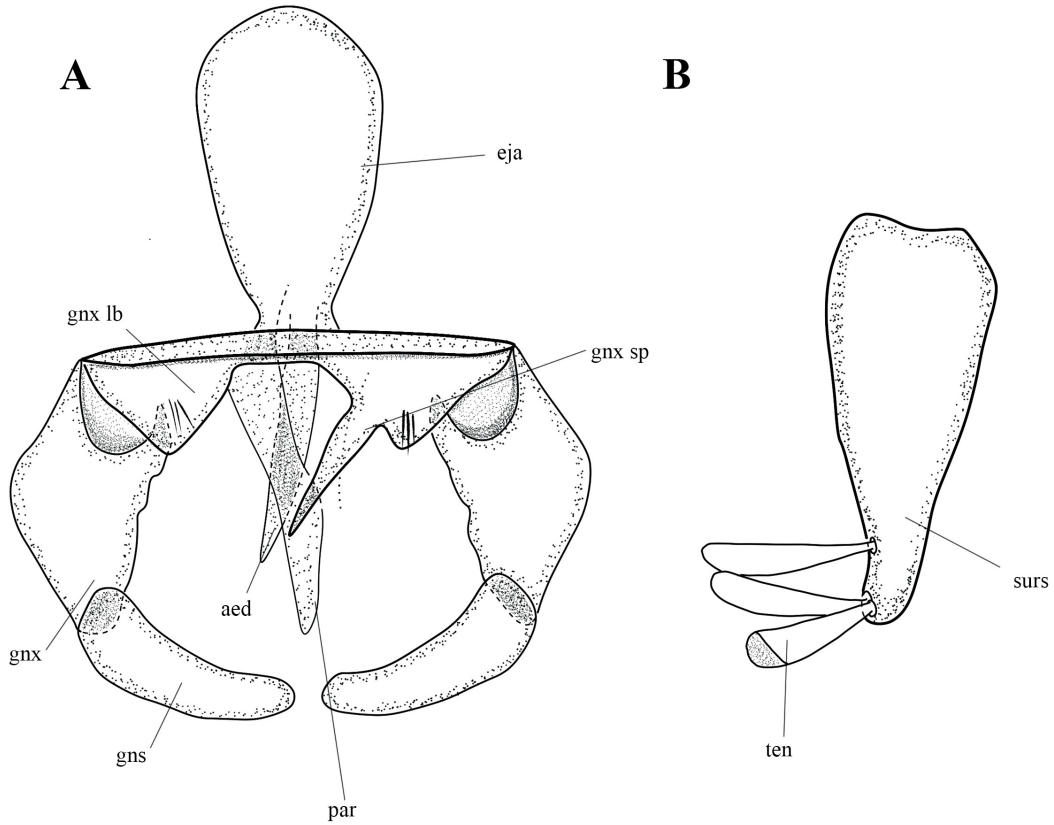

Fig. 23. *Bryopharsos tritaleum* Quate, 1996, ♂. **A**. Terminalia (ventral view). **B**. Surstyli. Abbreviations: aed = aedeagus; eja = ejaculatory apodeme; gns = gonostylus; gnx = gonocoxite; gnx lb = gonocoxal lobes; gnx sp = spine of gonocoxal lobe; par = paramere; surs = surstyli; ten = tenacula. No scales available. Figures adapted from Quate (1996).

Distribution

Brazil (Bravo & Araújo 2019) (Fig. 1).

DNA barcodes

No specimens were available for DNA extraction.

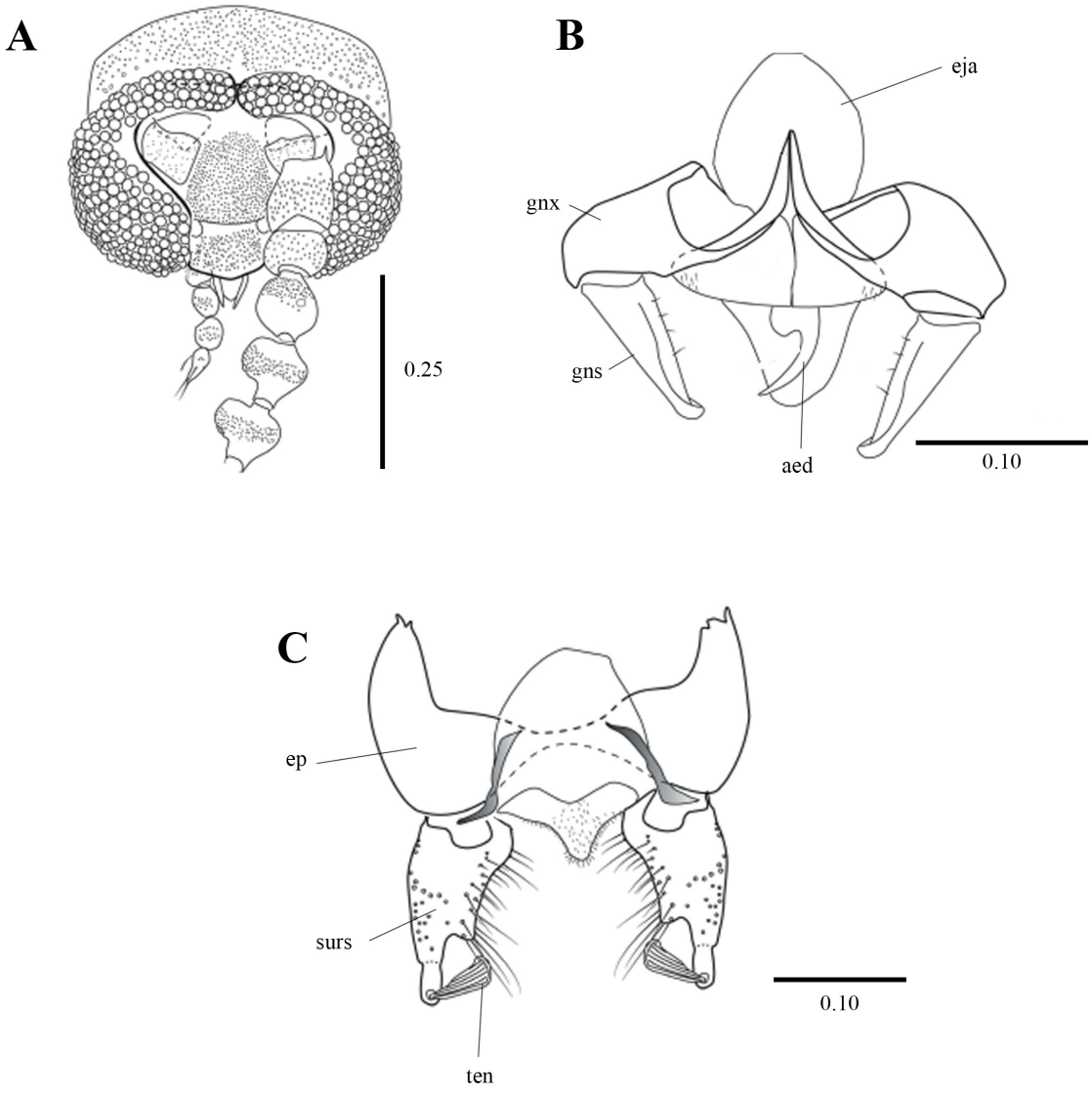

Fig. 24. *Bryopharsos uncinatum* Bravo & Araujo, 2019, ♂. **A**. Head. **B**. Terminalia (ventral view). **C**. Epandrium and surstyli. Abbreviations: aed = aedeagus; eja = ejaculatory apodeme; ep = epandrium; gns = gonostylus; gnx = gonocoxite; surs = surstyli; ten = tenacula. All scale bars are in millimeters. Figures adapted from Bravo & Araujo (2019) with permission of the copyright holder © Magnolia Press.

Identification key to the males of **Bryopharsos**

1. Gonostyli bifurcate ..... ***B. bifidum*** Jaume-Schinkel sp. nov.
– Gonostyli not bifurcate, digitiform 2

2. Surstyli with one tenaculum (Fig. 13B–C) 3
– Surstyli with two to seven tenacula (Figs 2C, 3A–D) 6

3. Eye bridge with five facet rows (as in Figs 19A); gonocoxal lobes with additional enlarged lobes (Fig. 19B); aedeagus blade-like (Fig. 19B); parameres clavate (Fig. 19B) .... ***B. paulistensis*** Bravo & Araújo, 2019
– Eye bridge with three or four facet rows (as in Fig. 6A); other characters variable 4

4. Eye bridge with three facet rows; gonostyli curved outwards (as in Fig. 13B, D); aedeagus digitiform and curved outwards (as in Fig. 13B, D) ..... ***B. curvum*** Jaume-Schinkel sp. nov.
– Eye bridge with four facet rows (Fig. 15A); gonostyli curved inwards; aedeagus variable 5

5. Aedeagus hook-shaped (Fig. 24B); paramere wide and triangular .... ***B. uncinatum*** Bravo & Araújo, 2019
– Aedeagus digitiform (as in Figs 15B, 16A); paramere digitiform (as in Figs 15B, 16A) .... ***B. insperatum*** Jaume-Schinkel sp. nov.

6. Surstyli with three to seven apical tenacula (Fig. 2C) 8
– Surstyli with only two apical tenacula (Figs 5, 8C, 9B) 7

7. Aedeagus digitiform, (Figs 4C, 5); paramere digitiform, longer than the aedeagus (Figs 4C, 5); some specimens present two tenacula on one surstylus and three on the other (as in Figs 4C, 5) .... ***B. asymmetricum*** Jaume-Schinkel sp. nov.
– Aedeagus digitiform with a rounded apex (Figs 8B, 9A); paramere digitiform, shorter than the aedeagus (Figs 8B, 9A); specimens always with two tenacula on each of the surstyli (Figs 8B, 9A) ..... ***B. bitenacula*** Jaume-Schinkel sp. nov.

8. Surstyli with four to seven apical tenacula (Fig. 20B) 10
– Surstyli with only three apical tenacula (Fig. 22C) 9

9. Aedeagus digitiform, curved (Fig. 22B, D), longer than paramere; surstyli with apical tenacula closely together (Fig. 22C) ..... ***B. tetracanthus*** Jaume-Schinkel sp. nov.
– Aedeagus digitiform, straight (Fig. 23A), shorter than paramere; surstyli with apical tenacula separated, two apically and one basally placed (Fig. 23B) ..... ***B. tritaleum*** Quate, 1996

10. Eye bridge with four facet rows; aedeagus digitiform, straight, about the same length as paramere (Fig. 12B); surstyli with four tenacula (Fig. 12C); tenacula of equal length .... ***B. clavigum*** Quate, 1996
– Eye bridge with four or five facet rows; aedeagus shape variable; length of aedeagus and paramere variable; surstyli with five to seven tenacula (Fig. 20B); tenacula length variable 11

11. Aedeagus digitiform, straight; aedeagus shorter than paramere; eye bridge with five face rows; surstyli with three or four apical tenacula (as in Fig. 17C); tenacula of equal length .... ***B. palpiculum*** Quate, 1996
– Aedeagus shape variable; length of aedeagus and paramere variable; eye bridge with four facet rows; surstyli with five, six, or seven apical tenacula; tenacula length variable 12

12. Aedeagus digitiform (Fig. 21); paramere strongly curved resembling an inverted 'J' (Fig. 21); surstyli with seven tenacula (Fig. 20B); tenacula of the same length ..... ***B. septenacula*** Jaume-Schinkel sp. nov.
– Aedeagus digitiform, straight; surstyli with five or six tenacula; tenacula length variable 13

13. Aedeagus digitiform, broader than the base of the paramere (Fig. 2C, see also Bravo & Araujo 2019: fig. 29); surstyli with five tenacula 15
– Aedeagus digitiform, narrower than the base of the paramere (Figs 11A, 14D); surstyli with six tenacula 14

14. Hypandrium shorter than aedeagal width; epandrium C-shaped ..... ***B. chuspi*** Jaume-Schinkel sp. nov.
– Hypandrium longer than aedeagal width; epandrium rectangular and not C-shaped ..... ***B. gorgona*** Jaume-Schinkel sp. nov.

15. All five tenacula of the same length (Fig. 2C); ejaculatory apodeme shorter than aedeagus ..... ***B. amazonensis*** Bravo & Araújo, 2019
– Tenacula of different lengths, four tenacula of equal length and one tenaculum shorter than others (Fig. 3C); ejaculatory apodeme about the same length as the aedeagus ..... ***B. claviformosum*** Quate, 1996

Analysis of DNA barcodes

All sequenced specimens form well-supported clusters (BS = 100) in the NJ tree (Fig. 25), matching morphological identifications. The maximum intraspecific uncorrected pairwise distance for the partial COI sequences of *B. amazonensis* were 0.32%, similarly, specimens of *B. claviformosum* had a maximum uncorrected pairwise distance of 0.16%, specimens of *B. palpiculum* had a maximum uncorrected pairwise distance 0.92%, and specimens of *B. septenacula* sp. nov. had a maximum uncorrected pairwise distance 0.45%. The interspecific uncorrected pairwise distance ranged from 16.62 to 19.51% between all the sequenced taxa.

Genus distribution model

Species distribution models calculated by MaxEnt show good model quality according to evaluation measures. MaxEnt shows comprehensible results according to our knowledge on climatic preferences of species inside the genus *Bryopharsos*. Of the 19 WorldClim variables, 13 were correlated, while only 6 were significant for the model construction. The variable that contributed most to the construction of this model was bio10 'Mean Temperature of Warmest Quarter' (73.1%), the second most important variable was bio11 'Mean Temperature of Coldest Quarter' (8.9%), meaning that temperature significantly conditions the distribution of this genus (Fig. 26).

According to the predictions, under current climatic conditions, the moth fly genus *Bryopharsos* is potentially established in much of the sub-humid to humid tropics and subtropics of America (Figs 1, 26). The modelled suitability of the climate for *Bryopharsos* aligns well with its known occurrences in tropical America between 23° N and 25° S. Therefore, areas with highly suitable climate conditions for *Bryopharsos* species include the Caribbean islands, most of Central America, the state of Tabasco in Mexico southward, and the Chocó-Darién biodiversity hotspot in Panama, western Colombia, and Ecuador. On the other hand, the model predicts a continuous distribution through the Andes mountain range in Ecuador and Colombia, to the Amazonian lowland forest region, from western Amazonia to central and northern Amazonia through Colombia, Ecuador, Venezuela, Peru, Amazonas, Acre and Rondonia states (Brazil) and northern Bolivia. A discontinuous distribution is observed in Amazonian

forest areas such as Guyanas and Pará. In addition, the model predicts moderately suitable conditions through the Atlantic forest patches along the coasts and in southern Brazil.

Discussion

Our results support comparison of DNA barcodes (COI sequences) as a good complementary tool for species identification in *Bryopharsos*, especially for morphologically similar species such as *B. amazonensis* and *B. claviformosum*. Our sequenced taxa form well-supported clusters as seen in the NJ tree (Fig. 25). Our DNA barcodes have a maximum intraspecific uncorrected pairwise distance of 0.92% (in *B. palpiculum*), a value similar to other known intraspecific distances within psychodine species, such as *Alepia viatrix* Jaume-Schinkel, Kvifte, Weele & Mengual, 2022 (5.75%), *Tonnoira chuki* Jaume-Schinkel, 2023 (1.87%), or *Platyplastinx ibanezbernali* Jaume-Schinkel & Kvifte, 2022 (1.35%) (Jaume-Schinkel *et al.* 2022; Jaume-Schinkel & Kvifte 2022; Jaume-Schinkel 2023). We, thus, believe that an integrative taxonomical approach, combining adult morphology and DNA barcoding, becomes a key component when discovering the number of species present in entomological samples.

The usage of the term surstyli (surstylus in singular) has been a long source of discussion in Psychodidae as different terms have been used to refer to the same caudal appendages (Curler & Moulton 2012). Furthermore, these appendages are non-homologous with those of the Eremoneura Lameere, 1906

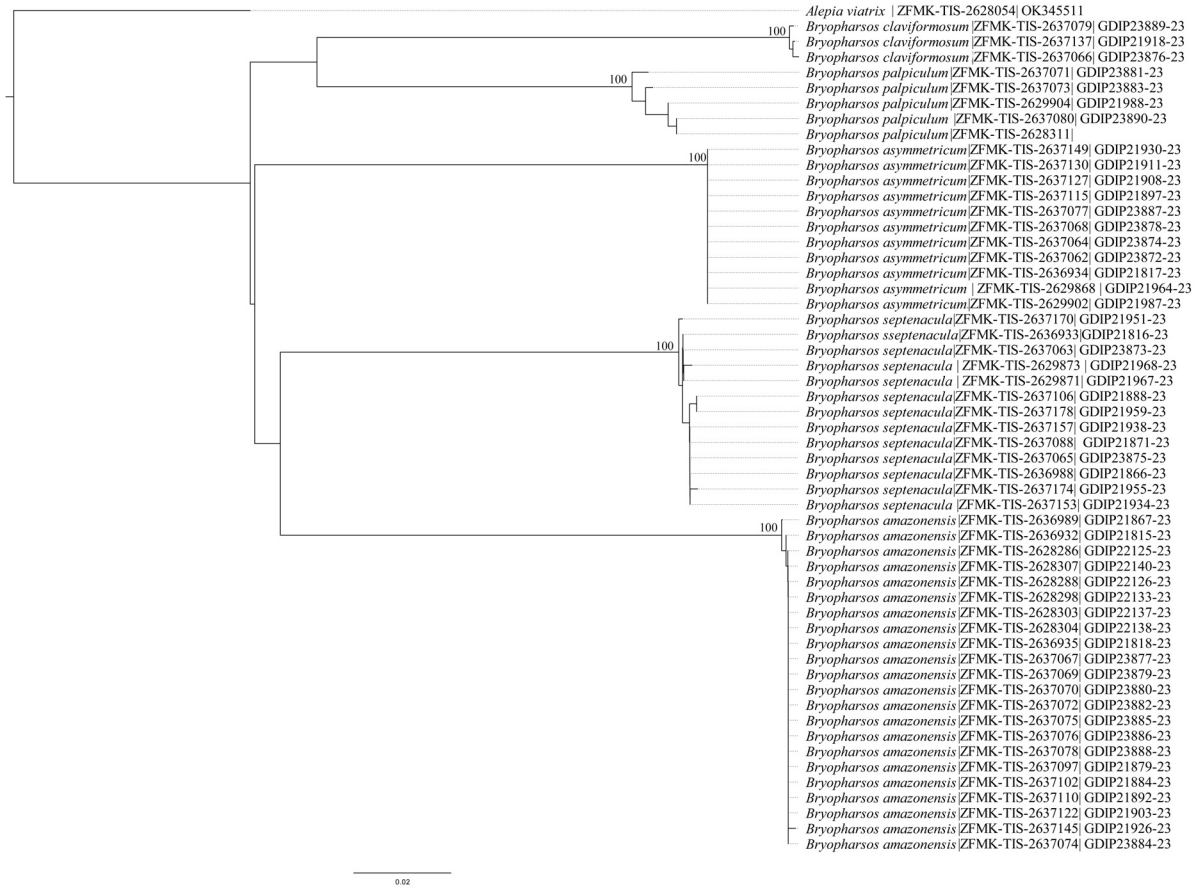

Fig. 25. Neighbor-Joining tree using Jukes-Cantor model based on the COI sequences of the examined material. The branch names for each specimen is composed by: the sample ID | Process ID or GenBank accession number. Bootstrap support values are given at the nodes.

(Cumming & Wood 2017); hence, some authors have referred to them as "epandrial lobes" (Sinclair *et al.* 2013), "epandrial claspers" (Santos & Curler 2014), "epandrial appendages" (Kvifte & Wagner 2017a), or "hypopods" (Kvifte & Wagner 2017b). According to Cumming & Wood (2017), the surstyli are apically clasping lobes derived from epandrium, and true surstyli are only present in the Eremoneura, whilst similar-looking appendages occur in a few nematocerous families (including Psychodidae) and some species of Psychodidae appear to have appendages originating from both the epandrium and proctiger (Kvifte & Wagner 2017b). Nevertheless, as shown in Fig. 3, the surstyli in the species of *Bryopharsos* seem to originate from the epandrium as articulate appendages; thus, we deem it appropriate to refer to the epandrial appendages with the term surstyli in the genus *Bryopharsos*. Nonetheless, further morphological data is desirable to understand the origin and functionality of these genital structures with the hope of finding common ground of the homology with other dipteran groups.

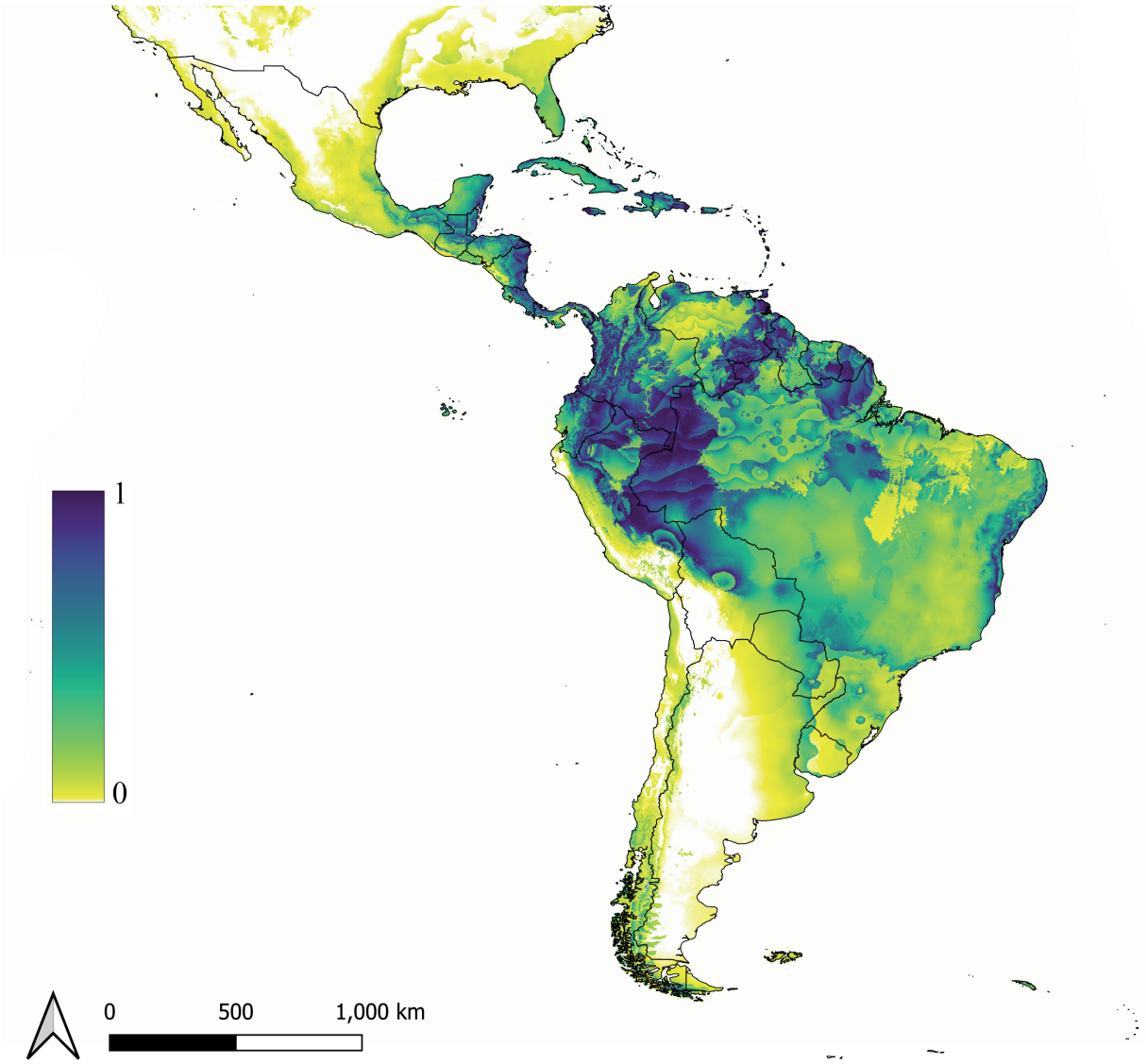

Fig. 26. Species distribution modeling map using MaxEnt 3.4.4. Outcome values from 0 (white) to 1 (dark blue) represent the relative probability of habitat suitability for the genus, with 0 indicating the least suitable areas and 1 indicating the most suitable areas.

We have noticed that when specimens are slide-mounted (i.e., Figs 2C, 4C), the aedeagus and paramere seem to originate from within the abdomen close to the ejaculatory apodeme. This perception changes with specimens that are not slide-mounted and examined with a SEM microscope (as in Fig. 3); the aedeagus seems to originate from within the abdomen piercing through the membrane of the gonocoxal apodeme (Fig. 3B, D [red color]) and the paramere seems to be part of the gonocoxal lobes membrane (Fig. 3B, D [blue color]). The male terminalia are composed of three-dimensional structures that are flattened during the slide preparation process, making them seem almost flat and two-dimensional. This distortion may lead to misinterpretation of characters and careful interpretation is advised.

The spine present in the gonocoxal lobes can vary in size and shape, even among individuals of the same species, and can be found on either side (left or right), or be completely absent. For instance, the majority of the examined material of *B. amazonensis* does not present the spine, but three individuals display it on the left side. Similarly, examined material of *B. septenacula* sp. nov. has a spine present either on the left or on the right side. Although the position of the spine is different in these species, the structure is similar and it seems that there is no broken spine on the other empty side of the gonocoxal lobes. If there were a spine on each side originally, we suppose that we could see the rest of the broken spine, and this is not the case. The function of the spine, as well as the variation of left/right placement, is unknown, and further study is required to clarify the possible reproductive function or evolutionary implications.

To date, *Bryopharsos* remains a genus present in the Neotropical Region only (Fig. 1). With the herein newly described species, the genus has 16 species. The herein-reported distribution of the species of *Bryopharsos* is restricted to seven countries: Brazil, Colombia, Costa Rica, Ecuador, Panama, Peru and Venezuela (Fig. 1). Nonetheless, our species distribution model (Fig. 26) predicts that the genus could be present in other areas of the American continent, including countries in South, Central, and North America. Moreover, our model also predicts the potential presence of *Bryopharsos* in Caribbean countries. The presence of known and undescribed species in more Neotropical countries is highly probable, and the lack of records can be derived from different socio-political scenarios, but we speculate it is mainly due to a lack of systematic collection and a lack of taxonomical expertise in those countries. Consequently, we encourage to carry on sampling across South, Central, and North America to gain a better understanding of the distribution of the species of *Bryopharsos*.

Acknowledgments

The present results are part of the genetic resources contract (research permit named “Estudio de la sistemática filogenética, taxonomía integrativa y genética de poblaciones de artrópodos terrestres del Ecuador continental”) (MAATE-DBI-CM-2024-0406) signed between the Ecuadorian Ministerio del Ambiente y Agua and the Instituto Nacional de Biodiversidad - INABIO. We are grateful to the two anonymous reviewers for their comments, which helped improve the final version of our publication. We also thank the editor, Torbjørn Ekrem, for his support. We extend our gratitude to Freddy Bravo for providing useful discussions of the species from Brazil. We are indebted to Björn Müller for performing the DNA extraction and PCR at ZFMK and for helping with the sequence upload to BOLD. SJS is thankful to Brian Brown, Giar-Ann Kung and Weiping Xie for hosting him during his visit to the LACM and is grateful with Greg Curler for the useful discussion regarding the genus, and to Greg and Amanda for hosting him during his visit. ICK is thankful to Victor Guagua Mosquera for letting us set up sampling traps on his farm and Emilio José Bernal for the logistics provided during field work.

References

Astrin J.J. & Stüben P.E. 2008. Phylogeny in cryptic weevils: molecules, morphology and new genera of western Palaearctic Cryptorhynchinae (Coleoptera: Curculionidae). *Invertebrate Systematics* 22: 503–522. https://doi.org/10.1071/IS07057

Bravo F. & Araújo M.X. 2019. Three new species of *Bryopharsos* Quate, 1996 (Diptera, Psychodidae, Psychodinae) from the Neotropical Region. *Zootaxa* 4619 (2): 364–370. https://doi.org/10.11646/zootaxa.4619.2.10

Cumming J.M. & Wood D.M. 2017. Adult morphology and terminology. *In*: Kirk-Springs A.H. & Sinclair B.J. (eds) *Manual of Afrotropical Diptera. Vol. 1. Introductory Chapters and Keys to Diptera Families*. Suricata 4: 89–133. South African National Biodiversity Institute, Pretoria.

Curler G.R. & Moulton J.K. 2012. Phylogeny of psychodid subfamilies (Diptera: Psychodidae) inferred from nuclear DNA sequences with a review of morphological evidence for relationships. *Systematic Entomology* 37: 603–616. https://doi.org/10.1111/j.1365-3113.2012.00634.x

Fick S.E. & Hijmans R.J. 2017. WorldClim 2: new 1-km spatial resolution climate surfaces for global land areas. *International Journal of Climatology* 37 (12): 4302–4315. https://doi.org/10.1002/joc.5086

Jaume-Schinkel S. 2023. Description of *Tonnoira chuki* sp. n. (Diptera: Psychodidae) from Ecuador with an updated taxonomical key for the genus *Tonnoira*. *Integrative Systematics* 6 (1): 51–57. https://doi.org/10.18476/2023.462484

Jaume-Schinkel S. & Kvite M.G. 2022. *Platyplastinx ibanezbernali* sp. nov., a new species of moth fly (Diptera: Psychodidae) from Ecuador. *Acta Entomologica Musei Nationalis Pragae* 62 (2): 383–389. https://doi.org/10.37520/aemnp.2022.020

Jaume-Schinkel S., Kvifte G. M., van der Weele R. & Mengual X. 2022. *Alepia viatrix* sp. nov. (Diptera: Psychodidae), a new species of a Neotropical genus found on the Azores Archipelago (Portugal). *Zootaxa* 5128 (3): 384–396. https://doi.org/10.11646/ZOOTAXA.5128.3.4

Ježek J. 2010. Further new taxa of non-biting moth flies (Diptera: Psychodidae: Psychodinae) from Malaysia. *Acta Entomologica Musei Nationalis Pragae* 50: 235–252.

Korbie D.J. & Mattick J.S. 2008. Touchdown PCR for increased specificity and sensitivity in PCR amplification. *Nature Protocols* 3: 1452–1456. https://doi.org/10.1038/nprot.2008.133

Kvifte G.M. 2018. Molecular phylogeny of moth flies (Diptera, Psychodidae, Psychodinae) revisited, with a revised tribal classification. *Systematic Entomology* 43: 596–605. https://doi.org/10.1111/syen.12288

Kvifte G.M. & Wagner R. 2017a. Psychodidae (Sand Flies, Moth Flies or Owl Flies). *In*: Kirk-Spriggs A.H. & Sinclair B.J. (eds) *Manual of Afrotropical Diptera. Volume 2. Nematocerous Diptera and Lower Brachycera*. Suricata 5607–632. South African National Biodiversity Institute, Pretoria.

Kvifte M.G. & Wagner R. 2017b. Review of *Neurosystasis* Satchell, with two new species from Cuba and a discussion of cerci and surstyli in Psychodinae (Diptera: Psychodidae). *Zootaxa* 4306 (1): 81–90. https://doi.org/10.11646/zootaxa.4306.1.4

Phillips S.J., Dudík M. & Schapire R.E. 2023. MaxEnt software for modeling species niches and distributions (Version 3.4.1). Available from http://biodiversityinformatics.amnh.org/open_source/maxent/ [accessed 8 Feb. 2023].

Quate L.W. 1996. Preliminary taxonomy of Costa Rican Psychodidae (Diptera), exclusive of Phlebotominae. *Revista de Biología Tropical* 44 (Supplement 1): 1–81.

Quate L.W. 1999. Taxonomy of Neotropical Psychodidae. (Diptera) 3. Psychodines of Barro Colorado island and San Blas, Panamá. *Memoirs on Entomology International* 14: 409–441.

Santos C.B. dos & Curler G.R. 2014. Four new species of *Tonnoira* Enderlein (Diptera: Psychodidae: Psychodinae) from the Brazilian Atlantic forest. *Zootaxa* 3760 (3): 463–470. https://doi.org/10.11646/zootaxa.3760.3.13

Saitou N. & Nei M. 1987. The neighbor-joining method: a new method for reconstructing phylogenetic trees. *Molecular Biology and Evolution* 4 (4): 406–425. https://doi.org/10.1093/oxfordjournals.molbev.a040454

Sinclair B.J., Cumming J.M. & Brooks S.E. 2013. Male terminalia of Diptera (Insecta): a review of evolutionary trends, homology, and phylogenetic implications. *Insect Systematics and Evolution* 44: 373–415. https://doi.org/10.1163/1876312X-04401001

Manuscript received: 17 April 2024
Manuscript accepted: 28 January 2025
Published on: 3 July 2025
Topic editor: Tony Robillard
Section editor: Torbjørn Ekrem
Desk editor: Radka Rosenbaumová